1956

Local buckling of wf shapes in the plastic range, Ph.D. Dissertation, Lehigh University, (1956)

G. Haaijer

Approved and recommended for acceptance as a dissertation in partial fulfillment of the requirements for the degree of Doctor of Philosophy.

3/28/56
(Date)

Bruno Thürlimann
Professor in Charge

Accepted, 4/13/56
(Date)

Special Committee directing the Doctoral work of Mr. Geerhard Haaijer

Chairman
Professor R. E. Kolm

Professor J. B. Hartmann

Professor G. E. Raynor

Professor B. Thürlimann

LOCAL BUCKLING OF WIDE-FLANGE SHAPES IN THE PLASTIC RANGE

by

Geerhard Haaijer

A DISSERTATION
Presented to the Graduate Faculty
of Lehigh University
in Candidacy for the Degree
of Doctor of Philosophy

Lehigh University

1956

A C K N O W L E D G M E N T S

The author is greatly indebted to Dr. Bruno Thürlimann who supervised the research project and was professor in charge of the present dissertation. His advice and suggestions are sincerely appreciated. The guidance of Professors R.E. Kolm, G.E. Raynor, and J.B. Hartman, Chairman and members respectively, of the Special Committee directing the author's doctoral work is gratefully acknowledged.

The project was part of the research program "Welded Continuous Frames and Their Components", carried out at Fritz Engineering Laboratory, Lehigh University, Bethlehem, Pennsylvania under the general direction of Dr. Lynn S. Beedle; the investigation is sponsored jointly by the Welding Research Council and the Department of the Navy with funds furnished by American Institute of Steel Construction, American Iron and Steel Institute, Column Research Council (Advisory), Office of Naval Research (Contract 39303), Bureau of Ships and Bureau of Yards and Docks. Professor William J. Eney is Director of Fritz Engineering Laboratory and Head of the Department of Civil Engineering.

The manuscript was typed by Misses Bernadine Krenicky and Patricia Torres and the drawings were prepared by Mr. Joseph C. Dilliard and Miss Etta Young. Their cooperation is sincerely appreciated.

TABLE OF CONTENTS

1. S Y N O P S I S

The application of plastic design to continuous frames constructed of wide-flange shapes, imposes more severe limitations on the geometry of these shapes than conventional elastic design. In regions where yielding starts first the flanges must be able to sustain strains considerably larger than the yield strain without the occurence of local (plate) buckling.

With this practical application in mind, the problem of buckling of steel plates compressed beyond the yield strain is treated in the present dissertation. In the strain-hardening range the material is considered to be homogeneous. However, because of the yielding process the material cannot be expected to remain isotropic. Therefore, general expressions for the buckling strength are derived assuming the material to have become orthogonally anisotropic.

Orthogonal anisotropy in the case of plane stress is expressed mathematically by stress-strain relations involving five moduli. Numerical values of the moduli are estimated from the incremental theory of plasticity taking the second invariant of the deviatoric stress tensor as the loading function. The influence of initial imperfections is taken into account through proper adjustment of the values of the moduli.

In the yielding range the average strain in the direction of loading is between the strain at which yielding starts and the strain at the beginning of strain-hardening. For this case the material

is considered to be partly elastic and partly strained up to the strain-hardening range.

Finally, theoretical estimates are compared with test results. Fair agreement is obtained.

2. INTRODUCTION

Presently used steel wide-flange shapes are proportioned such that no local buckling occurs within the elastic range. Consequently they can safely be used for structures in which the design is based upon theoretical first yield as the limiting condition (conventional design). However, design based upon ultimate strength (plastic design) imposes more severe requirements on the sections with regard to local buckling. The structure will reach its full ultimate load only if those parts where yielding starts first, can undergo sufficiently large deformations. For framed structures constructed of wide-flange shapes the flanges at the above mentioned locations must then be able to sustain strains considerably larger than the yield strain. Consequently the flanges should be proportioned such that local (plate) buckling does not occur under this condition.

In order to solve problems of plate buckling the relationships between the increments of stresses and strains due to the deflection of the plate out of its plane must be known. Within the elastic range the assumption that the material is isotropic and homogeneous leads to predictions which are in good agreement with test results(1)*. A satisfactory transition curve for the range from the elastic limit stress to the yield stress can easily be obtained by applying Bleich's semi-rational theory to an effective stress-strain curve(2).

\- - - - - - - - - - - -

* See list of references, page 49 .

During the yielding process the material is heterogeneous. Yielding takes place in so-called slip bands and the strain jumps from its value at the elastic limit to that at the beginning of strain-hardening(3). When all the material has been strained to the strain-hardening range the material again becomes homogeneous. To the strain-hardening range, stress-strain relations of different theories of plasticity could be applied. Such theories can be divided into two groups: deformation or total stress-strain relations and incremental stress-strain relations.

Bijlaard(4) was first to apply deformation stress-strain relations to the plate buckling problem. The theory was developed further by Ilyushin(5) and modified by Stowell(6). Incremental stress-strain relations were applied by Handelman and Prager(7). An extensive survey of stress-strain relations in the plastic range has been made by Drucker(8). Although the necessity for an incremental type of mathematical theory of plasticity has been shown, the results of plastic buckling tests on aluminum plates are well correlated by a deformation theory and bear no resemblance to predictions of incremental theory. Onat and Drucker(9) investigated the influence of initial imperfections on torsional buckling for a simplified model of a cruciform section. For this case the paradox appears at its worst. Onat and Drucker showed that incremental plasticity leads to proper results when unavoidable initial imperfections are taken into account.

All theories of plate buckling in the plastic range imply orthotropic behavior of the material. This assumption seems to be

very reasonable. Therefore, in the present dissertation general expressions for the buckling strength of orthotropic plates are derived from general stress-strain relations involving five moduli (Chapter 3). Tests by the author on combined compression and torsion of steel tubes showed that the behavior of the material is well described by the incremental theory with the second invariant of the deviatoric stress tensor as the loading function[10]. Consequently, this theory is used in order to obtain values of the moduli of the general stress-strain relations.

Generalities on stress and strain and incremental stress-strain relations are reviewed in Chapters 4 and 5. The influence of initial imperfections is illustrated in Chapter 6. From the results of coupon tests numerical values of the moduli are then obtained in Chapter 7. The influence of initial imperfections is taken into account through adjustment of the value of the shear modulus. Combining the results of Chapters 3 and 7 gives numerical solutions of the local buckling problem presented in Chapter 8. Theoretical predictions are compared with test results in Chapter 9.

3. BUCKLING OF RECTANGULAR ORTHOTROPIC PLATES

3.1 General

Consider a rectangular steel plate taking the center plane of the plate as the x - y coordinate plane. Compressing the plate in the x - direction into the strain-hardening range may affect all deformation properties of the material. Hence the tangent moduli, E_x and E_y in the x - and y - direction respectively, are probably different. The same may hold for the coefficients of dilatation, ν_x and ν_y in the x - and y - direction. The shear modulus, G_t, may also be affected.

Thus

$$\frac{\partial \epsilon_x}{\partial \sigma_x} = \frac{1}{E_x} \qquad \frac{\partial \epsilon_y}{\partial \sigma_y} = \frac{1}{E_y}$$

$$\frac{\partial \epsilon_x}{\partial \sigma_y} = -\frac{\nu_y}{E_y} \qquad \frac{\partial \epsilon_y}{\partial \sigma_x} = -\frac{\nu_x}{E_x} \qquad \ldots \qquad (3.1)$$

$$\frac{\partial \gamma_{xy}}{\partial \tau_{xy}} = \frac{1}{G_t}$$

where

ϵ = normal strain

γ = shear strain

σ = normal stress

τ = shear stress

Then the relations between the increments of strains and stresses can be written as follows:

$$d\epsilon_x = \frac{1}{E_x} d\sigma_x - \frac{\nu_y}{E_y} d\sigma_y$$

$$d\epsilon_y = -\frac{\nu_x}{E_x} d\sigma_x + \frac{1}{E_y} d\sigma_y \qquad (3.2)$$

$$d\gamma_{xy} = \frac{1}{G_t} d\tau_{xy}$$

If equations (3.2) are valid for the entire cross-section the expressions for the bending and twisting moments in terms of the deflection, w, in the direction of the z-axis become

$$M_x = -\frac{E_x I}{1-\nu_x \nu_y}\left[\frac{\partial^2 w}{\partial x^2} + \nu_y \frac{\partial^2 w}{\partial y^2}\right] \qquad (3.3)$$

$$M_y = -\frac{E_y I}{1-\nu_x \nu_y}\left[\frac{\partial^2 w}{\partial y^2} + \nu_x \frac{\partial^2 w}{\partial x^2}\right] \qquad (3.4)$$

$$M_{xy} = -2G_t I \frac{\partial^2 w}{\partial x \partial y} \qquad (3.5)$$

where

$$I = \frac{t^3}{12}$$

t = thickness of plate.

The condition that the bent position is in equilibrium can be expressed by the following differential equation:

$$D_x \frac{\partial^4 w}{\partial x^4} + 2H \frac{\partial^4 w}{\partial x^2 \partial y^2} + D_y \frac{\partial^4 w}{\partial y^4} = - t\sigma_x \frac{\partial^2 w}{\partial x^2} \quad . \quad . \quad (3.6)$$

where

$$D_x = \frac{E_x I}{1 - \nu_x \nu_y}$$

$$D_y = \frac{E_y I}{1 - \nu_x \nu_y}$$

$$D_{xy} = 2G_t I$$

$$2H = \nu_y D_x + \nu_x D_y + 2D_{xy}$$

The derivation of these equations may be found in the pertinent literature[11]. Only if $H^2 = D_x D_y$, an assumption made by Bleich[2], can solutions of this differential equation be easily obtained.

If the plate is initially perfectly plane the value of σ_x at which bifurcation of equilibrium occurs (the plane and the bent position are both equilibrium positions) is determined by equation (3.6). The condition that both the plane and the bent position are equilibrium positions can also be expressed in terms of work. The additional work done by the external forces due to bending of the plate must equal the change in internal energy of the plate.

This yields the following integral equation

$$\sigma_x t \iint \left|\frac{\partial w}{\partial x}\right|^2 dxdy = \iint \left[D_x \left|\frac{\partial^2 w}{\partial x^2}\right|^2 + \right.$$

$$+ D_y \left|\frac{\partial^2 w}{\partial y^2}\right|^2 + (\gamma_x D_y + \gamma_y D_x) \left|\frac{\partial^2 w}{\partial x^2}\right| \cdot \left|\frac{\partial^2 w}{\partial y^2}\right| +$$

$$\left. + 2D_{xy} \left|\frac{\partial^2 w}{\partial x \partial y}\right|^2 \right] dxdy \quad . \quad . \quad (3.7)$$

When external restraints are provided to the plate the right-hand side of equation (3.7) has to be supplemented by additional terms expressing the work done by these restraints.

By assuming an appropriate deflection surface, equation (3.7) gives an approximate solution. The degree of approximation depends upon the correctness of the assumed deflection surface. In any case the result will be conservative.

3.2 Plates with one Free Edge

For a rectangular plate with the loaded edges $x = 0$ and $x = \ell$ hinged, edge $y = 0$ restrained against rotation and edge $y = b$ free (figure 1) the following deflection surface is assumed

$$w = \left[A \frac{y}{b} + B \left\{ \left|\frac{y}{b}\right|^2 + a_1 \left|\frac{y}{b}\right|^3 + a_2 \left|\frac{y}{b}\right|^4 \right\} \right] \sin \frac{\pi x}{\ell} \quad . \quad . \quad (3.8)$$

The ratio B/A depends upon the amount of restraint. In the case of elastic restraint, where γ = moment per unit length required for a unit rotation

$$\beta = \frac{B}{A} = \frac{\gamma b}{2D_y} \quad . \quad . \quad . \quad . \quad . \quad . \quad (3.9)$$

Deflection surface (3.8) is similar to the one used by Lundquist and Stowell[12]. As shown in the appendix better results are obtained with equation (3.8) if the following values for a_1 and a_2 are used

For $0 < \beta < 0.3$ $\quad a_1 = -0.7$, $\quad a_2 = 0.2$

and for $\beta = \infty$ $\quad a_1 = -1.11$, $\quad a_2 = 0.57$

Substituting w in equation (3.7) and integrating gives

$$\sigma_x = \frac{t^2}{12(1-\nu_x\nu_y)}\left[E_x\left(\frac{\pi}{\ell}\right)^2 + E_y\left(\frac{1}{b}\right)^4 \cdot \left(\frac{\ell}{\pi}\right)^2 \cdot \frac{2\beta + \beta^2 C_3}{\frac{1}{3} + \beta C_1 + \beta^2 C_2} + \right.$$

$$- (\nu_y E_x + \nu_x E_y)\left(\frac{1}{b}\right)^2 \cdot \frac{\beta C_4 + \beta^2 C_5}{\frac{1}{3} + \beta C_1 + \beta^2 C_2} +$$

$$\left. + 4(1-\nu_x\nu_y) G_t \left(\frac{1}{b}\right)^2 \cdot \frac{1 + \beta C_6 + \beta^2 C_7}{\frac{1}{3} + \beta C_1 + \beta^2 C_2}\right] \quad . \quad . \quad (3.10)$$

where

$$C_1 = 1/2 + 2/5\, a_1 + 1/3\, a_2$$

$$C_2 = 1/5 + 1/3\, a_1 + 1/7\,(a_1^2 + a_2) + 1/4\, a_1 a_2 + 1/9\, a_2^2$$

$$C_3 = 4 + 12a_1^2 + 144/5\, a_2^2 + 12a_1 + 16a_2 + 36a_1 a_2$$

$$C_4 = 1 + 2a_1 + 3a_2$$

$$C_5 = 2/3 + 2a_1 + 1/5\ (6a_1^2 + 14a_2) + 3a_1a_2 + 12/7\ a_2^2$$

$$C_6 = 2(1 + a_1 + a_2)$$

$$C_7 = 4/3 + 3a_1 + 1/5\ (9a_1^2 + 16a_2) + 4a_1a_2 + 16/7\ a_2^2$$

The minimum value, σ_{cr}, of σ_x is obtained for ℓ/b given by

$$\frac{\ell}{b} = \pi \sqrt[4]{\frac{\frac{1}{3} + \beta C_1 + \beta^2 C_2}{2\beta + \beta^2 C_3}} \cdot \sqrt[4]{\frac{E_x}{E_y}} \quad . \quad . \quad . \quad (3.11)$$

In the limiting cases when the edge y = 0 is hinged or completely fixed equation (3.10) reduces to

a. Edge y = 0 hinged ($\beta = 0$) and $\ell = L$

$$\sigma_{cr} = \left(\frac{t}{b}\right)^2 \left[\frac{\pi^2 E_x}{12(1-\nu_x \nu_y)} \left(\frac{b}{L}\right)^2 + G_t\right] \quad . \quad . \quad (3.12)$$

For a long plate the first term can be neglected and

$$\sigma_{cr} = \left(\frac{t}{b}\right)^2 G_t \quad . \quad . \quad . \quad . \quad . \quad . \quad (3.13)$$

b. Edge y = 0 completely fixed ($\beta = \infty$)

The minimum value, σ_{cr}, of σ_x is obtained when the half-wave length ℓ satisfies

$$\frac{\ell}{b} = 1.39 \sqrt[4]{\frac{E_x}{E_y}} \quad . \quad . \quad . \quad . \quad . \quad . \quad (3.14)$$

Then

$$\sigma_{cr} = \left(\frac{t}{b}\right)^2 \left[\frac{10.14\sqrt{E_xE_y} - 3.88\ (\nu_y E_x + \nu_x E_y)}{12(1-\nu_x \nu_y)} + 1.82\ G_t\right]$$

$$. \quad . \quad . \quad (3.15)$$

3.3 Plates Supported Along All Four Edges

The loaded edges x = 0 and x = ℓ are hinged and the edges y = $\pm$ d/2 have equal restraint against rotation (figure 2). For this case the following deflection surface is used[13]

$$w = \left[B\pi\left(\frac{y^2}{d^2} - \frac{1}{4}\right) + (A + B) \cdot \cos\frac{\pi y}{d}\right]\sin\frac{\pi x}{\ell} \quad . \quad . \quad (3.16)$$

The ratio B/A depends on the amount of restraint. For elastic restraints with ψ = moment per unit length required for unit rotation

$$\beta = \frac{B}{A} = \frac{\psi d}{2D_y} \quad . \quad . \quad . \quad . \quad . \quad . \quad (3.17)$$

Substituting w from equation (3.16) in equation (3.17) and integrating gives

$$\sigma_x = \frac{t^2\pi^2}{12(1-\nu_x\nu_y)}\left[E_x\left(\frac{1}{\ell}\right)^2 + E_y \cdot \frac{\ell^2}{d^4} \cdot \frac{\frac{1}{4} + (c_1 + \frac{2}{\pi^2})\beta + \beta^2 c_3}{1/4 + \beta c_1 + \beta^2 c_2} + \right.$$

$$+ (\nu_y E_x + \nu_x E_y) \cdot \left(\frac{1}{d}\right)^2 \cdot \frac{1/4 + \beta c_1 + \beta^2 c_4}{1/4 + \beta c_1 + \beta^2 c_2} +$$

$$\left. + 4(1-\nu_x\nu_y)\cdot G_t\left(\frac{1}{d}\right)^2 \cdot \frac{1/4 + \beta c_1 + \beta^2 c_4}{1/4 + \beta c_1 + \beta^2 c_2}\right] \quad . \quad . \quad . \quad (3.18)$$

with

$c_1 = 0.09472$

$c_2 = 0.00921$

$c_3 = 0.04736$

$c_4 = 0.01139$

The minimum value of σ_x is obtained for ℓ given by

$$\frac{\ell}{d} = \sqrt[4]{\frac{E_x}{E_y} \frac{1/4 + \beta C_1 + \beta^2 C_2}{1/4 + (C_1 + 2/\pi^2)\beta + \beta^2 C_3}} \quad . \quad . \quad . \quad . \quad (3.19)$$

In the limiting cases, when the unloaded edges $y = \pm d/2$ are hinged or completely fixed, the minimum values of σ_x are

a. Edges $y = \pm d/2$ hinged ($\beta = 0$)

$$\sigma_{cr} = \frac{\pi^2}{12} \left(\frac{t}{d}\right)^2 \left[\frac{2\sqrt{E_x E_y} + \nu_y E_x + \nu_x E_y}{1 - \nu_x \nu_y} + 4G_t\right] . \quad . \quad (3.20)$$

where

$$\frac{\ell}{d} = \sqrt[4]{\frac{E_x}{E_y}} \quad . \quad . \quad . \quad . \quad . \quad . \quad . \quad . \quad . \quad . \quad . \quad . \quad (3.21)$$

b. Edges $y = \pm d/2$ completely fixed ($\beta = \infty$)

$$\sigma_{cr} = \frac{\pi^2}{12} \left(\frac{t}{d}\right)^2 \left[\frac{4.554\sqrt{E_x E_y} + 1.237\,(\nu_x E_y + \nu_y E_x)}{1 - \nu_x \nu_y} + \right.$$

$$\left. + 4.943\, G_t\right] \quad . \quad . \quad . \quad . \quad . \quad . \quad . \quad . \quad . \quad . \quad . \quad (3.22)$$

where

$$\frac{\ell}{d} = 0.66 \sqrt[4]{\frac{E_x}{E_y}} \quad . \quad . \quad . \quad . \quad . \quad . \quad . \quad . \quad . \quad . \quad . \quad . \quad (3.23)$$

In the following chapters values of E_x, E_y, ν_x, ν_y and G_t will be determined. On substituting these values in the above general expressions, numerical solutions to the local buckling problem will be obtained.

4. STRESS AND STRAIN

4.1 General

The moduli of the orthotropic stress-strain relations of equations (3.2) will be determined using the mathematical theory of plasticity. After summarizing generalities on stress and strain in the present chapter a review of the theory will be given in Chapter 5. In order to save space and time tensor notation will be used in referring to generalized stress and strain.

In tensor notation cartesian coordinates x_1, x_2 and x_3, corresponding to the x, y and z axis of engineering notation are denoted by letter subscripts i, j, k, l, which take the values 1, 2 and 3.

The nine components of stress and strain tensors are represented by single symbols σ_{ij} and ϵ_{ij} respectively. By definition

$$\begin{pmatrix} \sigma_{11} & \sigma_{12} & \sigma_{13} \\ \sigma_{21} & \sigma_{22} & \sigma_{23} \\ \sigma_{31} & \sigma_{32} & \sigma_{33} \end{pmatrix} \equiv \begin{pmatrix} \sigma_x & \tau_{xy} & \tau_{xz} \\ \tau_{yx} & \sigma_y & \tau_{yz} \\ \tau_{zx} & \tau_{zy} & \sigma_z \end{pmatrix} \quad . \quad . \quad . \quad (4.1)$$

and

$$\begin{pmatrix} \epsilon_{11} & \epsilon_{12} & \epsilon_{13} \\ \epsilon_{21} & \epsilon_{22} & \epsilon_{23} \\ \epsilon_{31} & \epsilon_{32} & \epsilon_{33} \end{pmatrix} \equiv \begin{pmatrix} \epsilon_x & 1/2\gamma_{xy} & 1/2\gamma_{xz} \\ 1/2\gamma_{yx} & \epsilon_y & 1/2\gamma_{yz} \\ 1/2\gamma_{zx} & 1/2\gamma_{zy} & \epsilon_z \end{pmatrix} \quad . \quad (4.2)$$

Due to symmetry of the tensors,

$$\sigma_{ij} = \sigma_{ji} \quad . \quad . \quad . \quad . \quad . \quad . \quad . \quad . \quad . \quad . \quad . \quad . \quad . \quad (4.3)$$

$$\epsilon_{ij} = \epsilon_{ji} \quad . \quad . \quad . \quad . \quad . \quad . \quad . \quad . \quad . \quad . \quad . \quad . \quad . \quad (4.4)$$

the stress and strain tensors each consist of 6 independent components. The derivation of equations (4.3) and (4.4) can be found in the pertinent literature, e.g. in Sokolnikoff's book on the mathematical theory of elasticity[14].

As is customary in tensor notation repeated subscripts will indicate summation. Furthermore, the Kronecker delta, δ_{ij}, is defined as unity for $i = j$ and zero for $i \neq j$.

The state of stress, with components σ_{ij} can be split into two parts: a uniform tension (or compression), s, and another state of stress, with components s_{ij}, having the same shear stress but zero mean normal stress. The latter is called the deviatoric stress tensor. Thus

$$\sigma_{ij} = s_{ij} + s\delta_{ij} \quad . \quad . \quad . \quad . \quad . \quad . \quad . \quad . \quad . \quad . \quad . \quad . \quad (4.5)$$

with

$$s = 1/3\ \sigma_{ii} \quad . \quad . \quad . \quad . \quad . \quad . \quad . \quad . \quad . \quad . \quad . \quad . \quad . \quad (4.6)$$

Similarly, the strain tensor with components ϵ_{ij} can be divided into a uniform expansion, e, and a deviatoric strain tensor with components e_{ij}.

Thus

$$\epsilon_{ij} = e_{ij} + e\delta_{ij} \quad . \quad . \quad . \quad . \quad . \quad . \quad . \quad . \quad . \quad . \quad . \quad (4.7)$$

and

$$e = 1/3\ \epsilon_{ii} \quad . \quad . \quad . \quad . \quad . \quad . \quad . \quad . \quad . \quad . \quad . \quad . \quad . \quad (4.8)$$

4.2 Invariants

The derivation of the principal stresses, σ_p, from the 6 independent components, σ_{ij}, of the stress tensor leads to a cubic equation

$$\sigma_p^3 + A\sigma_p^2 + B\sigma_p + C = 0 \quad . \quad . \quad . \quad . \quad . \quad . \quad . \quad . \quad (4.9)$$

The coefficients A, B and C are functions of the stress components. As equation (4.9) must be independent of the arbitrarily chosen coordinate axis, x_i, the coefficients A, B and C are necessarily invariants. It is customary to choose as the first invariant

$$I_1 = \sigma_{kk} \ (= -A) \quad . \quad . \quad . \quad . \quad . \quad . \quad . \quad . \quad . \quad . \quad . \quad (4.10)$$

With regard to plastic deformations the deviatoric stress tensor is more important than the stress tensor itself. The invariants specifying the state of deviatoric stress are obtained from a cubic equation similar to equation (4.9).

$$S_p^3 + A' S_p^2 + B' S_p + C' = 0 \quad . \quad . \quad . \quad . \quad . \quad . \quad . \quad . \quad (4.11)$$

The invariants are

$$J_1 = s_{kk} = \sigma_{kk} - s\,\delta_{kk} = 0 \quad . \quad . \quad . \quad . \quad . \quad . \quad . \quad (4.12)$$

$$J_2 = 1/2\, s_{ij}\, s_{ij} \quad (= -B') \qquad (4.13)$$

$$J_3 = 1/3\, s_{ij}\, s_{jk}\, s_{ki} \quad (= -C') \qquad (4.14)$$

4.3 Yield Conditions

It is commonly assumed that yielding occurs whenever some function of stress, $f(\sigma_{ij})$, equals some number, k. If the material is originally isotropic this yield condition is independent of the orientation of the coordinate system. In this instance f must be a function of the stress invariants. Bridgman[15] has investigated the influence of I_1 and found that pressures of the order of the yield stress have practically no influence on yielding. The yield condition thus becomes

$$f(J_2\, J_3) = k \qquad (4.15)$$

One of the simplest yield conditions is the Huber-von Mises-Hencky criterion

$$J_2 = k^2 \qquad (4.16)$$

where k denotes the yield stress in pure shear. It represents a surface of constant distortional strain energy. Nadai pointed out that it is also a constant octahedral shear stress criterion.

Tresca's maximum shear stress criterion is mathematically more complicated and takes the form

$$4J_2^3 - 27J_3^2 - 36k^2J_2^2 + 96k^4J_2 - 64k^6 = 0 \qquad (4.17)$$

However, as mentioned by Prager[16], even under the most unfavorable circumstances the value of $\sqrt{J_2}$ furnished by Tresca's yield condition differs from the value of k furnished by the Mises condition only by about 15%. Furthermore, test results usually fall in between the predictions of Tresca's and Mises' yield conditions. On account of its greater simplicity the Mises condition is generally preferred for theoretical analysis.

5. INCREMENTAL STRESS-STRAIN RELATIONS

5.1 General

An extension of the yield function is obtained by assuming the existence of a loading function, f (σ_{ij}), which depends upon the state of stress and strain and the history of loading. For ideally plastic materials plastic flow occurs whenever f equals some number k. For materials exhibiting strain-hardening plastic deformations occur when the loading function exceeds k.

Prager[17] proved that, if

1. A loading function exists
2. The relation between infinitesimals of stress and strain is linear,

the only permissible stress-strain relation for strain-hardening material when loading is

$$d\epsilon_{ij}^{p} = F \frac{\partial f}{\partial \sigma_{ij}} \frac{\partial f}{\partial \sigma_{kl}} d\sigma_{kl} \quad \ldots\ldots\ldots\ldots (5.1)$$

↑ This is letter l, not number 1.

and when unloading is

$$d\epsilon_{ij}^{p} = 0 \quad \ldots\ldots\ldots\ldots\ldots\ldots (5.2)$$

where ϵ_{ij}^{p} = plastic component of strain ϵ_{ij} and F and f are functions of ~~(stress and strain.)~~ strain and stress, respectively.

The geometric proof of Prager's stress-strain law (equations 5.1 and 5.2) is also included by Drucker in his survey of stress-strain relations in the plastic range[8].

Applying different types of loading functions Edelman and Drucker[18] have derived various incremental stress-strain relations from Prager's law.

As no information was available concerning the actual behavior of steel in the strain-hardening range the author carried out a few tests on combined compression and torsion of steel tubes[10]. The tubes were compressed into the strain-hardening range and then subjected to torsion while keeping the axial load constant. It was found that for this particular loading path the behavior is very well described by Prager's incremental stress-strain relations taking $f = J_2$.

Although these tests are by no means a general verification of this theory they give some indication of its possible validity. In view of these results and on account of its simplicity, the loading function $f = J_2$ will be applied in the following derivations.

5.2 Loading Function $f = J_2$

Applying the loading function $f = J_2$ to equations (5.1) and (5.2)

$$d\epsilon^p_{ij} = F\, s_{ij}\, dJ_2 \quad . \quad . \quad . \quad . \quad . \quad . \quad . \quad . \quad . \quad . \quad (5.3)$$

when $dJ_2 > 0$

$$d\epsilon_{ij}^{p} = 0 \quad \text{when} \quad dJ_2 \leq 0 \qquad (5.4)$$

The increments of the elastic components, ϵ_{ij}^{e}, of the strains are given by Hooke's law

$$d\epsilon_{ij}^{e} = \frac{1+\nu}{E} d\sigma_{ij} - \frac{\nu}{E} d\sigma_{kk} \delta_{ij} \qquad (5.5)$$

where

E = modulus of elasticity

ν = Poisson's ratio

For the case of plane stress ($\sigma_z = \tau_{xz} = \tau_{yz} = 0$) the stress-strain relations, written in unabridged form, are

$$d\epsilon_x = \frac{1}{E} d\sigma_x - \frac{\nu}{E} d\sigma_y + \frac{1}{3} F (2\sigma_x - \sigma_y) dJ_2 \qquad (5.6)$$

$$d\epsilon_y = -\frac{\nu}{E} d\sigma_x + \frac{1}{E} d\sigma_y + \frac{1}{3} F (2\sigma_y - \sigma_x) dJ_2 \qquad (5.7)$$

$$d\epsilon_z = -\frac{\nu}{E} (d\sigma_x + d\sigma_y) - \frac{1}{3} F (\sigma_x + \sigma_y) dJ_2 \qquad (5.8)$$

$$d\gamma = \frac{2(1+\nu)}{E} d\tau + 2F\tau dJ_2 \qquad (5.9)$$

when

$$dJ_2 = \frac{1}{3} (2\sigma_x - \sigma_y) d\sigma_x + \frac{1}{3} (2\sigma_y - \sigma_x) d\sigma_y + 2\tau d\tau > 0 \qquad (5.10)$$

and

$$d\epsilon_x = \frac{1}{E} d\sigma_x - \frac{\nu}{E} d\sigma_y \qquad (5.11)$$

$$d\epsilon_y = -\frac{\gamma}{E} d\sigma_x + \frac{1}{E} d\sigma_y \quad . . . . . (5.12)$$

$$d\epsilon_z = -\frac{\gamma}{E} (d\sigma_x + d\sigma_y) \quad . . . . . (5.13)$$

$$d\gamma = \frac{2(1+\gamma)}{E} d\tau \quad . . . . . (5.14)$$

when $dJ_2 \leq 0$

The function F can be obtained from the results of a simple coupon test for which $\sigma_y = \tau = d\sigma_y = d\tau = 0$

Denoting

$$\frac{d\sigma_x}{d\epsilon_x} = E_t \quad . . . . . (5.15)$$

F is defined by equation (5.6) as

$$F = \frac{3}{4J_2} \left[\frac{1}{E_t} - \frac{1}{E} \right] \quad . . . . . (5.16)$$

Because of initial imperfections the above derived stress-strain relations cannot be applied without modification to the local buckling problem. After investigating the influence of initial imperfections on two simplified models in Chapter 6, effective stress-strain relations for the strain hardening range of steel will be derived in Chapter 7.

6. INFLUENCE OF INITIAL IMPERFECTIONS

6.1 General

A perfectly plane plate will remain plane if it is subjected to loads acting in its center plane which do not exceed the corresponding buckling loads. In the case of longitudinal loading in the x-direction producing a state of stress with σ_x as the only component, this state of stress will remain unchanged up to the point when buckling occurs. Consequently the buckling stress can be obtained from stress-strain relations (5.6) to (5.9) with $\sigma_y = \tau = 0$.

However, the buckling strength of actual plates with unavoidable imperfections does not agree with the predictions for perfectly plane plates. The reason for the discrepancy seems to be equation (5.9) which predicts elastic behavior with regard to the superimposed shear stresses.

Applying a simplified stress-strain diagram to a simplified model of a cruciform section Onat and Drucker[9] have shown that small unavoidable imperfections may account for the difference between predicted and actual behavior. Apparently the influence of imperfections on sections which fail by torsional buckling is completely different from those which fail in bending. The latter case has been investigated by Wilder, Brooks and Mathauser[19].

In the following, this difference in behavior will be illustrated for simplified models which buckle in the strain-hardening range. The applied simplified stress-strain curve with $n = E/E_t = 40$ is shown in figure 3. Reasons why the compressive stresses can exceed the yield stress, σ_o, will be discussed in Chapter 7.

6.2 Simplified WF Column

The simplified WF column consists of two thin flanges of equal area separated by a web of infinite shear stiffness and negligible area (figure 4). Instead of a true initial imperfection the deflections at the beginning of strain-hardening ($\sigma = \sigma_o$ and $\epsilon = \epsilon_o$) are used in the computations.

Following the same approach as Wilder, Brooks and Mathauser the deflection curve is assumed to be

$$y = \bar{y} \sin \frac{\pi x}{\ell} \quad . \quad . \quad . \quad . \quad . \quad . \quad . \quad . \quad . \quad . \quad . \quad (6.1)$$

At the beginning of strain-hardening

$$y_o = \bar{y}_o \sin \frac{\pi x}{\ell} \quad . \quad . \quad . \quad . \quad . \quad . \quad . \quad . \quad . \quad . \quad . \quad (6.2)$$

The load vs deflection curve is found by considering equilibrium of the center section of the column.

For the first part of the load vs deflection curve the strain in both flanges increases and the relation between average stress and deflection is given by

$$\frac{\sigma}{\sigma_o} = \frac{\sigma_t}{\sigma_o} - \left(\frac{\sigma_t}{\sigma_o} - 1\right)\frac{f_o}{f} \quad \ldots\ldots\ldots (6.3)$$

where

σ = average stress of both flanges

σ_t = tangent modulus stress

$\sigma_t = \dfrac{\pi^2 E_t}{(\ell/r)^2}$

$f = \bar{y}/d$

d = depth of section

f_o = value of f at beginning of strain-hardening.

Strain reversal occurs for

$$f = f_s = \sqrt{\frac{1}{2}\left(1 - \frac{\sigma_o}{\sigma_t}\right)}\, f_o \quad \ldots\ldots\ldots (6.4)$$

The corresponding stress, σ_s, is obtained from equation (6.3) substituting $f = f_s$.

After strain-reversal has started the load vs deflection relation is given by

$$\frac{\sigma}{\sigma_o}\left[\frac{n-1}{2(n+1)} + f\right] = \frac{\sigma_s}{\sigma_o}\left[\frac{n-1}{2(n+1)} + f_s\right] + \frac{\sigma_t}{\sigma_o}\frac{2n}{n+1}(f - f_s) \quad \ldots\ldots (6.5)$$

Figure 6 shows curves of σ/σ_o vs f for $\sigma_t/\sigma_o = 1.2$ and different values of f_o. The figure illustrates the behavior of the

column for loads corresponding to stresses $\sigma \cong \sigma_t$. Although the deflections start to increase more rapidly the load continues to increase. Therefore it is safe to use the tangent modulus load, which corresponds to $\sigma = \sigma_t$, as the limit of usefulness of the column.

6.3 Simplified Cruciform Section

In contrast to the above example the influence of initial imperfections on the buckling strength of a column of simplified cruciform cross-section will now be illustrated. The simplified stress-strain curve of figure 3 is applied to the solution of the problem as given by Onat and Drucker[9].

The cross-section consists of a thin shell of constant thickness h (figure 5). The column which is loaded uniformly is assumed to fail by twisting. The ends are considered as providing no restraint, which considerably simplifies the kinematics of the problem and makes the state of stress and strain the same at each cross-section.

The shear stress follows the contour and is constant in magnitude. The resulting moment, M_1, is given by

$$M_1 = 8 \tau t b h \quad . . . . . (6.6)$$

The twisting moment, M_2, produced by the axial force is

$$M_2 = \sigma I_p \theta \quad . . . . . (6.7)$$

in which

I_p = polar moment of inertia

θ = angle of twist per unit length.

The condition that the column is in equilibrium is satisfied by equating M_1 and M_2 such that

$$\sigma = \frac{3t}{b^2} \cdot \frac{\tau}{\theta} \quad \ldots\ldots\ldots\ldots\ldots\ldots \quad (6.8)$$

The relationship between the increments of the stresses and angle of twist is found by differentiating equation (6.8)

$$d\sigma = \frac{3t}{b^2}\left(\frac{d\tau}{\theta} - \frac{\tau d\theta}{\theta^2}\right) \quad \ldots\ldots\ldots\ldots\ldots\ldots \quad (6.9)$$

Substituting equations (6.9), (6.8) and (5.6) in equation (5.9) leads to the following differential equation:

$$2\psi \frac{d\sigma}{d\psi} + \sigma\left[\frac{1/n' + \psi}{1 + \psi}\right] = \frac{\sigma_c^e}{n'} \quad \ldots\ldots\ldots\ldots\ldots\ldots \quad (6.10)$$

where

$$\psi = \frac{b^4}{3t^2}\theta^2$$

$$n' = \frac{3G}{E_t} + 1 - \frac{3G}{E}$$

$$\sigma_c^e = \frac{3t^2}{b^2} G \quad \text{(elastic torsional buckling stress)}$$

An approximate solution for small values of ψ is given by Onat and Drucker as

$$\sigma = \frac{\sigma_o\left(\frac{\psi_o}{\psi}\right)^{\frac{1}{2n'}} + \sigma_c^e\left[1 - \left(\frac{\psi_o}{\psi}\right)^{\frac{1}{2n'}}\right]}{1 + \frac{(n' - 1)}{2n}(\psi - \psi_o)} \quad \ldots\ldots\ldots\ldots \quad (6.11)$$

where ψ_o is the value of ψ at $\sigma = \sigma_o$, $\epsilon = \epsilon_o$.

Results for the strain-hardening range of steel, $n' = 46$ ($n = 40$) are shown in figure 7. Load vs rotation curves are plotted for initial imperfections $b\theta_o = 0$, 0.01^o and 0.1^o, $b\theta$ being the angle of twist between two cross-sections a distance b apart. In all cases $\sigma_c^e/\sigma_o = 5$.

It is seen that very small imperfections cause a considerable reduction of the column strength. A perfectly straight member would reach its elastic buckling load, for the case considered $\sigma_c^e/\sigma_o = 5$. An imperfection at $\sigma = \sigma_o$ and $\epsilon = \epsilon_o$ of $b\theta_o = 0.01^o$ reduces the maximum load to $\sigma_m/\sigma_o = 1.4$. Consequently the application of the J_2 incremental theory to a perfectly plane plate which fails primarily by twisting cannot be expected to correctly predict the buckling strength of actual plates.

Rather than attempt to solve the buckling problem of a plate with initial imperfections, effective stress-strain relations are determined in the next chapter. It will be necessary to reduce the initially elastic value of the tangent shear modulus such, that the application of stress-strain relations (5.6) to (5.9) to the general expressions of Chapter 3 will result in a correct description of the behavior of actual plates.

7. STRESS-STRAIN RELATIONS FOR THE STRAIN-HARDENING RANGE OF STEEL

7.1 Results of Coupon Tests

A typical stress-strain curve obtained from a simple coupon test is shown in figure 8. It must be borne in mind that the strain represents an average strain measured over a certain gage length. It would be entirely erroneous to assume that the local strains within the plastic range from ϵ_f to ϵ_o are equal to the average strain. Yielding of mild steel occurs in small slip bands[3]. Slip takes place in a "jump" such that the strain across such a narrow band jumps from ϵ_f to ϵ_o. The first slip band originates at a weak point in the specimen, due to an inclusion, a stress concentration or other defects. From there on yielding will spread along the specimen.

This consideration leads to the conclusion that there is no material within the specimen at a strain between the yield strain, ϵ_f, and the strain-hardening strain, ϵ_o. Either the material is still elastic or it has reached the strain-hardening range.

In the strain-hardening range, $\epsilon > \epsilon_o$, the material is again homogeneous and in this range the J_2 theory of plasticity will be applied. In the intermediate range, $\epsilon_f < \epsilon < \epsilon_o$, the specimen can be considered to consist of two materials.

The results of 21 compression coupon tests carried out at Fritz Engineering Laboratory are summarized in Table 1. The coupons were cut from the flanges of WF shapes and from angles. For the interpretation of the results of coupon tests the following must be taken into account. Coupons are tested continuously in a hydraulic testing machine. It has become customary in Fritz Laboratory to test coupons with a valve opening of the machine corresponding to a strain rate of 1 micro in./in. per second in the elastic range. It has been shown by Huber and Beedle[26] that the ratio of the yield stress of a static test (where the load settles down after each increment of strain) and the yield stress of a continuous coupon test is approximately 0.925. Consequently a value of the yield stress, σ_o, of 0.925 x 39.2 = 36 ksi will be used in the following derivations.

Stress-strain curves for the strain-hardening range as obtained from 5 selected coupon tests have been replotted in figure 9. Coupons 9 and 18 represent the extreme cases while 5, 15, and 17 represent tests with average results.

The average stress-strain curve for the strain-hardening range can be expressed by the three parameters introduced by Ramberg and Osgood[21].

$$\epsilon - \epsilon_o = \frac{\sigma - \sigma_o}{E_o} + K\left(\frac{\sigma - \sigma_o}{E_o}\right)^n \quad . \quad . \quad . \quad . \quad . \quad . \quad . \quad (7.1)$$

where

σ_o = 36 ksi

ϵ_o = 14 x 10^{-3} in./in.

E_o = 900 ksi *

K = 21

n = 2

Equation (7.1) is also plotted in figure 9.

The total stress-strain curve, as it will be used in the following derivations, is shown in figure 10. The tangent modulus, E_t, in the direction of loading, x, is defined by equation (5.15) and plotted in figure 11. This information is sufficient to determine F (J_2) defined by equation (5.16). From equations (5.16) and (7.1) it follows that

$$F = \left[67.3 \frac{1}{\sqrt{J_2}} - 593 \frac{1}{J_2}\right] \times 10^{-6} \frac{in^6}{kips^3} \quad . \quad . \quad . \quad (7.2)$$

for $J_2 > 1/3\ \sigma_o^2 = 432\ kips^2/in.^4$

Figure 12 shows F as a function of J_2.

Compression tests on coupons taken from webs of WF shapes have also been performed by Huber and Beedle[20]. The results showed that the yield stress of web material is in general about 10% higher

* The values of E_o in Table 1 are taken from F. L. reports in which they are usually not given as the slope of the stress-strain curve at the initiation of strain-hardening but as the slope at a strain somewhat larger than ϵ_o. Consequently E_o as used in equation (7.1) is larger than the average value given in Table 1.

than that of flange material. Unfortunately these compression tests were not carried into the strain-hardening range, and consequently no information is available with regard to the shape of the stress-strain curve in the strain-hardening range.

Results of tension coupon tests carried out as part of F. L. Project 205E (see Table 2) show the same tendency of higher yield stresses for web material. The strain-hardening modulus, E_o, however, does not seem to be affected. Consequently the only difference of the stress-strain curves for flange and web material is assumed to be in the value of σ_o. For flanges σ_o = 36 ksi and for webs σ_o = 40 ksi.

7.2 The Tangent-Modulus In Shear

Consider the case where shear stresses, τ, are superimposed on a constant normal stress, σ_x, taking $\sigma_y = 0$ and $d\sigma_x = d\sigma_y = 0$. The relations between the increments of stress and strain given by equations (5.6) and (5.9) reduce to

$$d\epsilon_x = \frac{4}{3} F \sigma_x \tau d\tau \quad . . . . . (7.3)$$

$$d\gamma = \frac{2(1+\nu)}{E} d\tau + 4F \tau^2 d\tau \quad . . . . . (7.4)$$

Integrating equation (7.4) gives the relationship between τ and γ as shown in figure 13 for σ_x = 36 ksi and σ_x = 48 ksi. The corresponding slope

$$G_t = \frac{d\tau}{d\gamma} \quad . . . . . (7.5)$$

is plotted in figure 14.

It should be noted that from equation (7.3) it follows that, due to the shear stress, τ, the axial strain, ϵ_x, increases (figure 15). This phenomenon has also been confirmed by tests[10]. Consequently when a plate fails by twisting, an increase of the axial load is carried by the central part of the plate cross-section and the shear stresses occur at the part of the section near the plate surfaces. Therefore, it is justified to assume $d\sigma_x = 0$ in determining G_t. Furthermore, in cases where G_t is of importance e.g. hinged outstanding flanges, normal stresses, σ_y, perpendicular to the direction of loading are small, justifying the assumption $\sigma_y = 0$.

It is seen from figure 14 that the value of G_t drops rapidly for small values of γ. However, from the point at which $G_t = 2000$ ksi the decrease is slower. Consequently this value is selected as a useful value of G_t for the strain-hardening range of steel. From figure 13 it follows that the influence of the magnitude of the normal stress can be neglected for that part of the strain-hardening range under consideration.

7.3 Bi-Axial Normal Stresses

For regions of a plate in which cross bending is of importance the shear stresses are zero or very small, e.g. the center of plates supported along all four edges or the fixed edge of a clamped outstanding flange.

In this case equations (5.6) and (5.7) reduce to

$$d\epsilon_x = \left[\frac{1}{E} + \frac{1}{9} F (2\sigma_x - \sigma_y)^2\right] d\sigma_x + \left[\frac{\nu}{E} - \frac{1}{9} F (2\sigma_x - \sigma_y)(2\sigma_y - \sigma_x)\right] d\sigma_y \quad . \quad . \quad . \quad (7.6)$$

$$d\epsilon_y = \left[\frac{1}{E} + \frac{1}{9} F (2\sigma_y - \sigma_x)^2\right] d\sigma_y + \left[\frac{\nu}{E} - \frac{1}{9} F (2\sigma_x - \sigma_y)(2\sigma_y - \sigma_x)\right] d\sigma_x \quad . \quad . \quad . \quad (7.7)$$

Comparing equations (7.6) and (7.7) with equations (3.2) gives

$$\frac{1}{E_x} = \frac{1}{E} + \frac{1}{9} F (2\sigma_x - \sigma_y)^2 \quad . \quad . \quad . \quad . \quad . \quad . \quad . \quad . \quad . \quad . \quad (7.8)$$

$$\frac{1}{E_y} = \frac{1}{E} + \frac{1}{9} F (2\sigma_y - \sigma_x)^2 \quad . \quad . \quad . \quad . \quad . \quad . \quad . \quad . \quad . \quad . \quad (7.9)$$

$$\nu_x = \frac{\frac{\nu}{E} - \frac{1}{9} F (2\sigma_x - \sigma_y)(2\sigma_y - \sigma_x)}{\frac{1}{E} + \frac{1}{9} F (2\sigma_x - \sigma_y)^2} \quad . \quad . \quad . \quad . \quad . \quad (7.10)$$

$$\nu_y = \frac{\frac{\nu}{E} - \frac{1}{9} F (2\sigma_x - \sigma_y)(2\sigma_y - \sigma_x)}{\frac{1}{E} + \frac{1}{9} F (2\sigma_y - \sigma_x)^2} \quad . \quad . \quad . \quad . \quad . \quad (7.11)$$

For a perfectly plane plate ($\sigma_y = 0$) equations (7.8) to (7.11) reduce to

$$E_x = E_t \quad . \quad . \quad . \quad . \quad . \quad . \quad . \quad . \quad . \quad . \quad . \quad . \quad . \quad . \quad . \quad (7.12)$$

$$E_y = \frac{4 E E_t}{E + 3E_t} \quad . \quad . \quad . \quad . \quad . \quad . \quad . \quad . \quad . \quad . \quad . \quad . \quad . \quad (7.13)$$

$$\nu_x = \frac{E - (1 - 2\nu)\, E_t}{2E} \quad . \quad . \quad . \quad . \quad . \quad . \quad . \quad . \quad . \quad . \quad (7.14)$$

$$\nu_y = \frac{2\, E - (1 - 2\nu)\, E_t}{E + 3\, E_t} \quad . \quad . \quad . \quad . \quad . \quad . \quad . \quad . \quad . \quad . \quad (7.15)$$

Equations (7.12) to (7.15) have been applied with different notation by Handelman and Prager[7].

Equations (7.9) to (7.11) are valid only if

$$dJ_2 > 0 \quad . \quad . \quad . \quad . \quad . \quad . \quad . \quad . \quad . \quad . \quad . \quad . \quad . \quad . \quad . \quad (7.16)$$

or rewritten

$$2d\sigma_x - d\sigma_y > 0 \quad . \quad . \quad . \quad . \quad . \quad . \quad . \quad . \quad . \quad . \quad . \quad . \quad . \quad (7.17)$$

and with equations (7.6) and (7.7)

$$(2 - \nu)\, d\epsilon_x - (1 - 2\nu)\, d\epsilon_y > 0 \quad . \quad . \quad . \quad . \quad . \quad . \quad . \quad (7.18)$$

Figure 16 shows the assumed linear strain distribution due to curvatures dK_x and dK_y in the x- and y- directions.

$$d\epsilon_x = d\epsilon_1 + z dK_x \quad . \quad . \quad . \quad . \quad . \quad . \quad . \quad . \quad . \quad . \quad . \quad . \quad (7.19)$$

$$d\epsilon_y = d\epsilon_2 + x dK_y \quad . \quad . \quad . \quad . \quad . \quad . \quad . \quad . \quad . \quad . \quad . \quad . \quad (7.20)$$

where $d\epsilon_1$ and $d\epsilon_2$ are strain increments of the central plane in the x and y direction and z is the distance to the central plane.

The condition that all of the section is deformed plastically is obtained by substituting equations (7.19) and (7.20) in equation (7.18)

$$(2 - \nu)\ (d\epsilon_1 + z dK_x) - (1 - 2\nu)\ (d\epsilon_2 + z dK_y) > 0 \quad . \quad . \quad (7.21)$$

for $-t/2 \leq z \leq t/2$

The increase of the force per unit width in the x- direction, N_x, is found by rearranging equation (3.2) and integrating over the thickness of the plate

$$dN_x = \int_{-t/2}^{t/2} (d\sigma_x)\ dz =$$

$$= \frac{E_x t}{1 - \nu_x \nu_y}\ (d\epsilon_1 + \nu_y\ d\epsilon_2) \quad . \quad . \quad . \quad . \quad . \quad . \quad (7.22)$$

The increase of the force per unit width in the y- direction is

$$dN_y = \int_{-t/2}^{t/2} (d\sigma_y)\ dz =$$

$$= \frac{E_y t}{1 - \nu_x \nu_y}\ (d\epsilon_2 + \nu_x\ d\epsilon_1) \quad . \quad . \quad . \quad . \quad . \quad . \quad (7.23)$$

However, no external forces are applied in the y- direction, thus

$$dN_y = 0 \quad . \quad . \quad . \quad . \quad . \quad . \quad . \quad . \quad . \quad . \quad . \quad . \quad . \quad (7.24)$$

or

$$d\epsilon_2 = -\nu_x\ d\epsilon_1 \quad . \quad . \quad . \quad . \quad . \quad . \quad . \quad . \quad . \quad . \quad . \quad . \quad (7.25)$$

Substituting equation (7.25) in (7.22) gives

$$dN_x = E_x t\ d\epsilon_1 \quad . \quad . \quad . \quad . \quad . \quad . \quad . \quad . \quad . \quad . \quad . \quad . \quad (7.26)$$

The plasticity condition, equation (7.21), then becomes

$$\left[2 - \nu + (1 - 2\nu) \nu_x \right] d\epsilon_1 + (2 - \nu)\, z dK_x - (1 - 2\nu)\, z dK_y > 0 \quad (7.27)$$

for $-t/2 \leq z \leq t/2$

If the neutral zone between loading and unloading zones is at $z = t/2$, equation (7.27) gives

$$d\epsilon_1 = \frac{t/2\left((2 - \nu)\, dK_x - (1 - 2\nu)\, dK_y\right)}{2 - \nu + (1 - 2\nu)\nu_x} \quad . \quad . \quad . \quad . \quad (7.28)$$

Obviously $d\epsilon_1 > 0$ only if

$$dK_y < \frac{2 - \nu}{1 - 2\nu}\, dK_x \quad . \quad . \quad . \quad . \quad . \quad . \quad . \quad . \quad . \quad . \quad . \quad (7.29)$$

Checking the plasticity condition (7.27) for $d\epsilon_1$ given by equation (7.21) shows that condition (7.27) is not violated if (7.29) is satisfied.

If the neutral zone is at $z = -t/2$ equation (7.27) gives

$$d\epsilon_1 = \frac{t/2\left((1 - 2\nu)\, dK_y - (2 - \nu)\, dK_x\right)}{2 - \nu + (1 - 2\nu)\nu_x} \quad . \quad . \quad . \quad . \quad (7.30)$$

and $d\epsilon_1 > 0$ only if

$$dK_y > \frac{2 - \nu}{1 - 2\nu}\, dK_x \quad . \quad . \quad . \quad . \quad . \quad . \quad . \quad . \quad . \quad . \quad . \quad (7.31)$$

The plasticity condition (7.27) is not violated if equation (7.31) is satisfied.

From equations (7.28) and (7.30) it is seen that

$$d\epsilon_1 = 0$$

and consequently according to equation (7.26)

$$dN_x = 0$$

for

$$dK_y = \frac{2 - \nu}{1 - 2\nu} dK_x \quad \ldots\ldots\ldots\ldots (7.32)$$

Furthermore $dJ_2 = 0$ for the entire cross-section. Thus

$$d\sigma_x = \frac{1}{2} d\sigma_y \quad \ldots\ldots\ldots\ldots (7.33)$$

for an initially plane plate with $\sigma_y = 0$.

In this case, since bending is not accompanied by an increase in axial load the influence of initial imperfections will be the greatest. Suppose biaxial loading starts at $\sigma_x = \sigma_x^*$, $\sigma_y = 0$, $\epsilon_x = \epsilon_x^*$, $\epsilon_y = \epsilon_y^*$. Then it follows from equation (5.10) with equation (7.33) that

$$dJ_2 = \frac{1}{2} \sigma_y d\sigma_y \quad \ldots\ldots\ldots\ldots (7.34)$$

Integrating (7.34) gives

$$J_2 = J_2^* + \sigma_y^2 = \frac{1}{3} \sigma_x^{*2} + \sigma_y^2 \quad \ldots\ldots\ldots\ldots (7.35)$$

Equations (7.8) to (7.11) reduce to

$$\frac{1}{E_x} = \frac{1}{E} + \frac{4}{9} F \sigma_x^{*2} \quad \ldots\ldots\ldots\ldots\ldots\ldots (7.36)$$

$$\frac{1}{E_y} = \frac{1}{E} + \frac{1}{9} F \left(\frac{3}{2}\sigma_y - \sigma_x^*\right)^2 \quad \ldots\ldots\ldots\ldots\ldots\ldots (7.37)$$

$$\nu_y = \frac{\frac{\nu}{E} - \frac{2}{9} F \sigma_x^* \left(\frac{3}{2}\sigma_y - \sigma_x^*\right)}{\frac{1}{E} + \frac{1}{9} F \left(\frac{3}{2}\sigma_y - \sigma_x^*\right)^2} \quad \ldots\ldots\ldots\ldots\ldots\ldots (7.38)$$

$$\nu_x = \frac{\frac{\nu}{E} - \frac{2}{9} F \sigma_x^* \left(\frac{3}{2}\sigma_y - \sigma_x^*\right)}{\frac{1}{E} + \frac{4}{9} F \sigma_x^{*2}} \quad \ldots\ldots\ldots\ldots\ldots\ldots (7.39)$$

The results are shown graphically in figures 17 and 18. From figure 17 it is seen that σ_y has little affect on E_x. Negative values of σ_y cause a drop of E_y as shown in the same figure. However, according to equation (7.24) negative values of σ_y must always be accompanied by positive values at other parts of the plate cross-section. For the latter case an increase of E_y is observed. Consequently, the effective modulus of the whole section will be affected only to a small extent. Furthermore, the product $\nu_x \cdot \nu_y$ does not change much because of σ_y (figure 18). Thus for biaxial bending the influence of initial imperfections is neglected.

The values of E_x, E_y, ν_x, and ν_y are given by equations (7.12) to (7.15). The results are plotted as functions of ϵ_x in figures 19 and 20.

Ex, see fig 11

8. APPLICATION TO LOCAL BUCKLING OF WIDE-FLANGE SHAPES

8.1 Outstanding Flanges of Infinite Length

The critical stress for an outstanding flange of an orthotropic material is given by equation (3.10). Substituting the values of the moduli derived in Chapter 7 into this equation, will give an estimate of the buckling strength of an actual steel flange. The ratio of the half wave length, ℓ, and the flange width, b, is given as a function of the coefficient of restraint, β, by equation (3.11) and is shown in figure 22. From figure 21 it is seen that $\sqrt[4]{E_y/E_x}$ varies from 1.38 for $\epsilon_x = 14 \times 10^{-3}$ to 1.40 for $\epsilon_x = 55 \times 10^{-3}$. Consequently $\sqrt[4]{E_y/E_x}$ has been chosen to have a constant value of 1.39 for the entire strain-hardening range. Finally the critical stress is obtained by combining equations (3.10) and (3.11).

As deformations are more important than stresses the results are plotted in figure 23 as ϵ_{cr} vs b/t curves, where ϵ_{cr} is the strain corresponding to the critical stress. The curves plotted are for $\beta = 0$ (hinged flange), $\beta = 0.01$, $\beta = 0.1$ and $\beta = \infty$ (fixed flange).

For the intermediate range, $\epsilon_f < \epsilon_{cr} < \epsilon_o$, yielding will start at certain locations and spread along the flange. Buckling will occur when a sufficient length has yielded to allow a buckle to be formed under the action of yield stress σ_o. The length of the

plastically deformed buckle will be finite and consequently the average strain of the infinitely long flange will approach the yield strain. The transition curves for $\epsilon_f < \epsilon_{cr} < \epsilon_o$ have therefore been indicated as vertical lines in figure 23.

8.2 Hinged Flanges of Finite Length

Consider a hinged flange of length 2L. The loaded edges x = 0 and x = 2L are fixed, the unloaded edge y = 0 is hinged and the unloaded edge y = b is free. If all of the material has been strained into the strain-hardening range, the buckling stress is given by equation (3.12).

In the elastic range equation (3.12) reduces to

$$\sigma_{cr} = \left(\frac{t}{b}\right)^2 \left[\frac{\pi^2 E}{12\ (1 - \nu^2)} \left(\frac{b}{L}\right)^2 + G \right] \quad . \quad . \quad . \quad . \quad . \quad (8.1)$$

When σ_{cr} obtained from equation (8.1) equals or exceeds σ_o yielding will have commenced. Assume that yielding starts at both ends and then moves toward the middle. This assumption seems to be reasonable in view of the fixed end restraints and has also been confirmed by tests.

The middle section, being still elastic, is practically rigid compared with the yielded zones of length ζL. Assuming that only the latter will deform equation (3.12) must be replaced by the following

$$\sigma_{cr} = \sigma_o = \left(\frac{t}{b}\right)^2 \left[\frac{\pi^2 E_x}{12(1 - \nu_x \nu_y)} \left(\frac{b}{\zeta L}\right)^2 + G_t \right] \quad . \quad . \quad (8.2)$$

The corresponding critical strain is

$$\epsilon_{cr} = (1 - \zeta)\,\epsilon_f + \zeta\,\epsilon_o \quad . \quad . \quad . \quad . \quad . \quad . \quad . \quad . \quad (8.3)$$

Substituting in equation (8.2) the values of E_x, ν_x, ν_y and G_t this equation determines the relationship between b/t and ζ. For L/b = 2.65 the b/t vs ζ curve has been plotted in figure 24 as a solid line. As elastic deformations have been neglected in equation (8.2) b/t = ∞ for ζ = 0. For this case b/t = 20.7 which is found from equation (3.12) by substituting the elastic values of E_x, ν_x, ν_y, G_t and taking σ = 36 ksi and L/b = 2.65. Knowing the rigid plastic solution and the point for ζ = 0 of the elastic-plastic solution the latter has been sketched in figure 24 as a dotted line. The elastic-plastic solution of b/t vs ζ with equation (8.3) gives ϵ_{cr} as a function of b/t for the range $\epsilon_f < \epsilon_{cr} < \epsilon_o$. The solution for $\epsilon_{cr} > \epsilon_o$ is found from equation (3.12).

8.3 Webs

The problem of buckling of uniformly compressed webs (rectangular plates supported at all four edges) has been treated theoretically in section 3.3. The critical stress is given by equation (3.18), the ratio of half-wave length, ℓ, to width of plate, d, being determined by equation (3.19).

Figure 26 shows a plot of ℓ/d as a function of the factor of restraint, β, for $\sqrt[4]{E_y/E_x}$ = 1.39, a value representative of the strain-hardening range. Substituting these values for ℓ/d in equation

(3.18) gives the values of the critical stress. The corresponding strains have been plotted in figure 27 as a function of the width over thickness ratio, d/t, for $\beta = 0$ and $\beta = \infty$.

Applying the same reasoning as in the case of infinitely long flanges (section 8.1) the transition curves for the range $\epsilon_f < \epsilon < \epsilon_o$ are found to be vertical lines in figure 27.

9. TEST RESULTS AND SUMMARY

9.1 Compression Tests on Angles

A number of compression tests on angles were performed with the purpose of checking the theoretical estimates developed above. Angle specimens have better known boundary conditions than WF sections and therefore give a more positive check. When buckling torsionally, the flanges of the angle act as two plates each with one free and one hinged edge, the heel forming the hinged edges. The loaded ends of the column were fixed against rotation in the testing machine. The dimensions of all specimens are given in table 3.

The resultant stress vs axial strain curves for the columns are shown in figure 28. Furthermore the rotations of the center sections were determined and are plotted as a function of the strain in figure 29. The critical strains are defined as the strain at which the rotation starts to increase more rapidly than it did initially. Specimens A41 and A42 did not buckle torsionally but failed by bending about the weak axis.

The results of all tests on angles are summarized in table 4. The critical strains are plotted as a function of the b/t ratios as in figure 25. In this figure the theoretical solution is also shown, the derivation of which is given in section 8.2. The test results compare favorably with the theoretical predictions.

9.2 Tests on Wide-Flange Shapes

In order to investigate the actual behavior of WF shapes with regard to local buckling, six different shapes were each tested under two loading conditions:

(a) Axial compression (Test D1, D2, D3, D4, D5, D6)

(b) Pure bending (Test B1, B2, B3, B4, B5, B6)

The dimensions of all WF specimens are given in table 5.

The length of each specimen was divided into three gage lengths over which the change in length was measured directly with 0.0001" Ames dials. Along the edges of the flanges and the center of the web lateral deflection measurements were taken. For the bending tests the lateral rotation was measured at the loading points (which were supported against lateral rotation) and near the center line of the beam.

The results of the compression and bending tests are shown in figures 30 and 31 respectively. Plotted are P/A vs ϵ_{av} for the compression tests and M/Z vs ϵ_{av} for the bending tests

P = compressive load

M = bending moment

A = area of cross-section

Z = plastic section modulus (twice the static moment of half the section about the strong axis)

ϵ_{av} = average strain at center of compressed flange.

As a typical example, the maximum flange and web deflections and lateral rotation vs the average strain for test B-3 are shown in figure 32. From these curves the crticial strains are obtained as indicated by arrows in figures 30 and 31. The critical strain is defined as the average strain at which the deflection of the flange or web starts to increase more rapidly than it did initially. The results of all tests are summarized in table 6.

When comparing the results of tests on WF shapes it should be borne in mind that the different types of buckling cannot be separated. Consequently the results should be interpreted with caution. For the cases where flange buckling was predominant the critical strains of the flanges vs the b/t ratios and the theoretical curves are plotted in figure 23. The results of tests D4 and D6 are omitted because web buckling occurred first and obviously caused premature flange buckling. Furthermore specimen B4 did not develop a major flange buckle but failed by lateral buckling. Therefore this result has also been eliminated from figure 23. From this figure it can be concluded that, if premature web buckling is prevented, the webs of the tested sections provide positive restraint to the flanges corresponding to a value of β of the order of 0.01.

For the cases where web buckling occurred first (Tests D2, D4 and D6) the critical strains are plotted vs the d/t ratios as in figure 27. This figure also shows the corresponding theoretical curves. For test D2 flange and web buckling occurred simultaneously

and it is therefore possible that the web buckled prematurely.

9.3 Summary

The results of the investigation presented in this dissertation can be divided into two parts: the derivation of stress-strain relations for the strain-hardening range of structural steel and their applications to the local buckling problem.

Incremental stress-strain relations were derived describing the orthotropic behavior of steel after it has been compressed into the strain-hardening range. The values of the tangent moduli and the coefficients of dilatation in the direction of compression and perpendicular to it are shown in figures 11, 19 and 20. An applicable value of the tangent shear modulus was found to be 2000 ksi. The above stress-strain relations were applied to the local buckling problem. The derived values of the moduli and coefficients were substituted in general expressions for the buckling strength of orthotropic plates. The agreement between predictions and test results (figures 23, 25 and 27) finally justified this approach.

A direct practical application of the findings presented in this dissertation is the prevention of local buckling of outstanding flanges in continuous frames, in which the design is based upon ultimate strength. From the required rotation capacity of the plastic hinges

the strains of the flanges can be determined. Figure 23 then gives the required b/t ratio, for $\beta = 0.01$. It should be emphasized, however, that the stress-strain relations could equally well be applied to other problems involving the occurrence of biaxial stresses and strains in the strain-hardening range of steel.

10. REFERENCES

1. Timoshenko, S., "THEORY OF ELASTIC STABILITY", McGraw-Hill, New York, 1936.

2. Bleich, F., "BUCKLING STRENGTH OF METAL STRUCTURES", McGraw-Hill, New York, 1952.

3. Nadai, A., "THEORY OF FLOW AND FRACTURE OF SOLIDS", McGraw-Hill, New York, 1950.

4. Bijlaard, P. P., "SOME CONTRIBUTIONS TO THE THEORY OF ELASTIC AND PLASTIC STABILITY", Pubs. Itern. Assoc. for Bridge and Structural Engineering, Vol. VIII, 1947.

5. Ilyushin, A. A., "STABILITY OF PLATES AND SHELLS BEYOND THE PROPORTIONAL LIMIT", (translated from Russian), NACA TM-116, October, 1947.

6. Stowell, E. Z., "A UNIFIED THEORY OF PLASTIC BUCKLING OF COLUMNS AND PLATES", NACA Report 898, 1948.

7. Handelman, G. H. and Prager, W., "PLASTIC BUCKLING OF A RECTANGULAR PLATE UNDER EDGE THRUSTS", NACA TN-1530, August, 1948.

8. Drucker, D. C., "STRESS-STRAIN RELATIONS IN THE PLASTIC RANGE -- A SURVEY OF THEORY AND EXPERIMENT", Report A11 S1, Graduate Division of Applied Mathematics, Brown University, December, 1950.

9. Onat, E. T. and Drucker, D. C., "INELASTIC INSTABILITY AND INCREMENTAL THEORIES OF PLASTICITY", Journal of the Aeronautical Sciences, Vol. 20, No. 3, March, 1953.

10. Haaijer, G., "COMBINED COMPRESSION AND TORSION OF STEEL TUBES IN THE STRAIN-HARDENING RANGE", Fritz Laboratory Report 241.1, Lehigh University (in preparation).

11. Girkmann, K., "FLACHENTRAGWERKE", 2nd Edition, Springer Verlag, Vienna, 1948.

12. Lundquist, E. E. and Stowell, E. Z., "CRITICAL COMPRESSIVE STRESS FOR OUTSTANDING FLANGES", NACA Report 734, 1942.

13. Lundquist, E. E. and Stowell, E. Z., CRITICAL COMPRESSIVE STRESS FOR FLAT RECTANGULAR PLATES SUPPORTED ALONG ALL EDGES AND ELASTICALLY RESTRAINED AGAINST ROTATION ALONG THE UNLOADED EDGES", NACA Report No. 733, 1942.

14. Sokolnikoff, I. S., "MATHEMATICAL THEORY OF ELASTICITY", McGraw-Hill, New York, 1946.

15. Bridgman, P. W., "FLOW AND FRACTURE", Trans. A. I. M. E., Iron and Steel Division, Vol. 162, 1945.

16. Prager, W., "THE STRESS-STRAIN LAWS OF THE MATHEMATICAL THEORY OF PLASTICITY", Transactions A.S.M.E., Vol. 70, Journal of Applied Mechanics, September, 1948.

17. Prager, W., "RECENT DEVELOPMENTS IN THE MATHEMATICAL THEORY OF PLASTICITY", Journal of Applied Physics, Vol. 20, Nr 3, 1949.

18. Edelman, F. and Drucker, D. C., "SOME EXTENSIONS OF ELEMENTARY PLASTICITY THEORY", Report A11-46/42, Graduate Division of Applied Mathematics, Brown University, January, 1950.

19. Wilder, T. W., III, Brooks, W. A., Jr., and Mathauser, E. E., "THE EFFECT OF INITIAL CURVATURE ON THE STRENGTH OF AN INELASTIC COLUMN", NACA TN 2872, January, 1953.

20. Huber, A. W. and Beedle, L. S., "RESIDUAL STRESS AND THE COMPRESSIVE STRENGTH OF STEEL", Welding Journal, 33 (12), December, 1954.

21. Ramberg, W. and Osgood, R., "DESCRIPTION OF STRESS-STRAIN CURVES BY THREE PARAMETERS", NACA TN 902, 1943.

11. N O M E N C L A T U R E

Tensor Notation

x_i	=	coordinate axis
i, j, k, ℓ, m		are letter subscripts taking the values 1, 2 and 3
σ_{ij}	=	components of stress tensor
σ_p	=	principal stress
s_{ij}	=	components of deviatoric stress tensor
s	=	mean normal stress
ϵ_{ij}	=	components of strain tensor
ϵ^e_{ij}	=	elastic strain component
ϵ^p_{ij}	=	plastic strain component
e_{ij}	=	components of deviatoric strain tensor
e	=	mean normal strain
δ_{ij}	=	Kronecker delta
I_1	=	first invariant of stress tensor
J_1, J_2 & J_3		are invariants of deviatoric stress tensor
f	=	yield and loading function
k	=	constant
F	=	function defined by equation (5.1)

Engineering Notation

x, y & z		are coordinate axis
w	=	deflection of plate
y	=	deflection of simplified column
$\bar{y}$	=	maximum value of y

f	=	ratio of $\bar{y}$ over depth of simplified column
f_o	=	value of f at initiation of strain-hardening
f_s	=	value of f at which strain reversal takes place
σ_x	=	normal stress in x direction
σ_x^*	=	value of σ_x at which biaxial loading starts
σ_y	=	normal stress in y direction
σ_o	=	yield stress
σ_t	=	tangent modulus stress
σ_{cr}	=	critical (buckling) stress
σ_{cr}^e	=	elastic buckling stress
σ_s	=	value of σ at which strain reversal takes place
τ_{xy}	=	shear stress
ϵ_x	=	normal strain in x direction
ϵ_x^*	=	value of ϵ_x at which biaxial loading starts
ϵ_y	=	normal strain in y direction
ϵ_y^*	=	value of ϵ_y at which biaxial loading starts
ϵ_o	=	strain at initiation of strain-hardening
ϵ_f	=	yield strain
ϵ_{cr}	=	critical strain corresponding to σ_{cr}
ϵ_{av}	=	average strain
γ_{xy}	=	angular strain in xy plane
E	=	modulus of elasticity
E_t	=	tangent modulus
E_x	=	tangent modulus in x direction
E_y	=	tangent modulus in y direction
E_o	=	strain-hardening modulus

G	=	modulus of elasticity in shear
G_t	=	tangent modulus in shear
ν	=	Poisson's ratio
ν_x	=	coefficient of dilatation for stress increment in x direction
ν_y	=	coefficient of dilatation for stress increment in y direction
n	=	exponent in equation (7.1)
n	=	ratio of modulus of elasticity over tangent modulus
n'	=	ratio defined by equation (6.10)
D_x	=	bending stiffness per unit width of plate in x direction
D_y	=	bending stiffness per unit width of plate in y direction
D_{xy}	=	torsional stiffness per unit width of plate
H	=	function defined by equation (3.6)
P	=	compressive load
M	=	bending moment
M_x	=	bending moment per unit width of plate in x direction
M_y	=	bending moment per unit width of plate in y direction
M_{xy}	=	torsional moment per unit width of plate
N_x	=	axial force per unit width of plate in x direction
N_y	=	axial force per unit width of plate in y direction
Q_y	=	shear force per unit width of plate
$\bar{Q}_y$	=	boundary shear force per unit width of plate
ℓ	=	half wave length of buckled shape
b	=	wdith of plate with one free edge
d	=	width of plate supported at all four edges

d = depth of simplified column

t = thickness of plate

I = moment of inertia per unit width of plate

A = area of cross-section

Z = plastic section modulus

h = thickness of sheet forming simplified cruciform section

θ = angle of twist per unit length

θ = lateral rotation of beam

ψ = edge moment per unit length to produce unit rotation of edge

Ψ = function defined by equation (6.10)

K_x = curvature of plate in x direction

K_y = curvature of plate in y direction

K_{xy} = twist of plate

$A, B, a_1, a_2, c_1, c_2, c_3, c_4, c_5, c_6, c_7, h_1$ and h_2 are constants

$\beta = B/A$ = coefficient of restraint

A P P E N D I X

Deflection Surfaces of Outstanding Flanges

In order to obtain an approximate solution for an orthotropic plate buckling problem, an assumed deflection surface may be used in the energy equation (3.7). When all edges are hinged, fixed or partially restrained against rotation an appropriate deflection surface fulfilling all boundary conditions can easily be found (Section 3.3).

However, when the plate has a free edge as in the case of outstanding flanges the selection of a surface becomes more involved. Consider a rectangular plate, the loaded edges $x = 0$ and $x = \ell$ hinged, the unloaded edge $y = 0$ either hinged, fixed or restrained and the unloaded edge $y = b$ free. The boundary conditions for the free edge are:

$$M_y = 0 \quad \ldots\ldots\ldots\ldots \quad (A.1)$$

$$\bar{Q}_y = Q_y + \frac{\partial M_{xy}}{\partial x} = 0 \quad \ldots\ldots\ldots\ldots \quad (A.2)$$

where

Q_y = shear per unit length

$\bar{Q}_y$ = boundary shear per unit length.

Q_y is found from equilibrium of a differential plate element

$$Q_y = \frac{\partial M_y}{\partial y} + \frac{\partial M_{xy}}{\partial x} \quad \ldots\ldots\ldots\ldots \quad (A.3)$$

The boundary shear $\bar{Q}_y$ is determined by replacing the twisting moment by equivalent shear forces and adding them to Q_y. The derivation of these equations can be found in the pertinent literature [11]. Substituting in equations (A1) and (A2) the expressions for M_y and M_{xy}, equations (3.4) and (3.5) give

$$\frac{\partial^2 w}{\partial y^2} + \gamma_x \frac{\partial^2 w}{\partial x^2} = 0 \quad \ldots \ldots \quad (A.4)$$

$$D_y \frac{\partial^3 w}{\partial y^3} + (\gamma_x D_y + 2 D_{xy}) \frac{\partial^3 w}{\partial x^2 \partial y} = 0 \quad \ldots \quad (A.5)$$

If edge y = 0 is hinged the following deflection surface satisfies the boundary conditions at all but the free edge

$$w = \left[\frac{y}{b} + h_1 \left(\frac{y}{b}\right)^3 + h_2 \left(\frac{y}{b}\right)^4 \right] \sin \frac{\pi x}{\ell} \quad \ldots \quad (A.6)$$

Substituting equation (A.6) in the boundary conditions for the free edge, i.e. equations (A4) and (A5), gives two equations from which the coefficients h_1 and h_2 can be determined. Figure 33 shows h_1 and h_2 as a function of ℓ/b for values of the rigidities corresponding to an axial strain of 25×10^{-3}. From the figure it is seen that for $\ell/b > 2$ the coefficients are approximately zero. It may be noted that for an elastic and isotropic material h_1 and h_2 also usually are taken zero.

When edge y = 0 is fixed deflection surface

$$w = \left[\left(\frac{y}{b}\right)^2 + a_1 \left(\frac{y}{b}\right)^3 + a_2 \left(\frac{y}{b}\right)^4 \right] \sin \frac{\pi x}{\ell} \quad \ldots \quad (A.7)$$

satisfies the boundary conditions at all edges except the free edge, $y = b$. Substituting w as given by (A7) in equations (A4) and (A5) yields two equations from which a_1 and a_2 can be determined. The result is shown in figure 34 where a_1 and a_2 are plotted as a function of ℓ/b for values of the rigidities corresponding to an axial strain of 25×10^{-3}. It is seen that the coefficients show little variation for the range $\ell/b > 2$.

For the case where the unloaded edge, $y = 0$, is restrained, a combination of equation (A6) and equation (A7) is used

$$w = \left[\frac{y}{b} + \beta\left\{\left(\frac{y}{b}\right)^2 + a_1\left(\frac{y}{b}\right)^3 + a_2\left(\frac{y}{b}\right)^4\right\}\right]\sin\frac{\pi x}{\ell} \quad . \quad . \quad (A.8)$$

For small values of β the half-wave length which corresponds to the minimum value of σ will satisfy the condition $\ell/b > 2$. For this range the following values of a_1 and a_2 have been selected

$$a_1 = -0.7$$

$$a_2 = 0.2$$

From figure 22 showing ℓ/b as a function of β it is seen that these values of a_1 and a_2 may be used for $\beta < 0.3$.

Applying these values to the case of a fixed flange ($\beta = \infty$) would give a value of half-wave length to flange width ratio of

$$\ell/b = 1.20$$

However, this value of ℓ/b is outside the range for which the above values of a_1 and a_2 are valid. By a trial and error procedure it is found that, for a fixed flange,

$$a_1 = -1.11$$

$$a_2 = 0.57$$

and $$\ell/b = 1.00$$

Lundquist and Stowell[12], in their paper on buckling of outstanding flanges, assumed the following deflection surface

$$w = \left[\frac{y}{b} + \beta \left\{ \left(\frac{y}{b}\right)^2 + a_1^* \left(\frac{y}{b}\right)^3 + a_2^* \left(\frac{y}{b}\right)^4 + a_3^* \left(\frac{y}{b}\right)^5 \right\} \right] \sin\frac{\pi x}{\ell} \quad \text{(A.9)}$$

with $$a_1^* = -1.0076$$

$$a_2^* = +0.5076$$

$$a_3^* = -0.1023$$

For small values of the coefficient of restraint, β, it will make little difference whether equation (A8) or (A9) is used. For $\beta = 0$ the result is identical. The biggest difference will occur for $\beta = \infty$. In this case the b/t ratio for which $\epsilon_{cr} = \epsilon_o$ obtained from equation (A9) would be b/t = 17.65. Using equation (A8) with $a_1 = -1.11$ and $a_2 = 0.57$ gives b/t = 14.6 for $\epsilon_{cr} = \epsilon_o$. Although equation (A9) is known to be good in the elastic range it can not be applied to the strain-hardening range of steel.

TABLE 1

RESULTS OF COMPRESSION COUPON TESTS

Coupon	Fritz Lab. Number	Section	σ_o ksi	ϵ_o x10^3	E_o ksi	Note
1	220A-UF3	14WF30	39.7	13.0	730	All WF section coupons taken from flanges
2	220A-UF4	"	41.5	14.6	690	
3	220A-LF1	"	42.5	14.6	650	
4	220A-LF2	"	39.0	12.5	790	
5	220A-LF3	"	39.7	12.5	730	
6	220A-LF4	"	42.0	13.0	670	
7	220A-A	"	40.8	15.0	640	
8	220A-B	"	40.8	12.5	675	
9	220A-D	"	40.3	15.5	650	
10	220A-E	"	39.6	14.5	650	
11	220A-F	"	35.3	(6.0)	780	
12	220A-G	"	36.2	(6.5)	700	
13	220A-B2F3	8WF31	40.0	17.4	770	
14	220A-B2F6	"	38.8	11.5	810	
15	220A-B2F7	"	39.0	14.8	730	
16	205E-C14	10WF33	40.0	14.5	855	
17	205E-C15	"	37.0	13.8	805	
18	205E-C2	8WF40	38.4	12.8	1060	
19	205E-C9	L6.6.3/8	39.0	12.8	710	
20	205E-C12	"	37.6	14.3	906	
21	205E-C13	"	35.1	14.6	845	
Average Values*			39.2	13.9	755	

* Numbers in parentheses not used for determining average value

TABLE 2

RESULTS OF TENSION COUPON TESTS

Coupon	Section	*Location	Yield Stress σ_o ksi	Strain at Strain-Hardening $\epsilon_o \times 10^3$	Strain-Hardening Modulus E_o ksi
T 6	10WF33	1	35.5	16.5	675
T 7		5	35.0	14.7	750
T 21		1	35.4	18.4	530
T 22	8WF24	2	35.6	18.0	600
T 23		3	36.3	19.3	470
T 31		1	35.6	14.3	525
T 32	10WF39	2	36.8	18.9	580
T 33		3	37.8	16.3	580
T 41		1	37.1	18.0	500
T 42	12WF50	2	36.9	18.1	530
T 43		3	39.4	15.9	580
T 51		1	37.6	16.9	560
T 52	8WF35	2	37.3	16.6	465
T 53		3	39.9	19.6	600
T 61		1	38.0	20.8	520
T 62	10WF21	2	34.2	23.4	570
T 63		3	44.2	23.6	490

*Location of Coupons

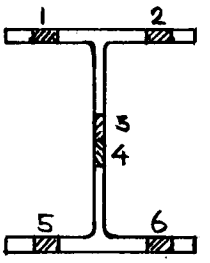

All coupons tested in Baldwin 60,000# Hydraulic Machine. Valve opening corresponding to testing speed of 1 micro-in./in. per sec. in the elastic range.

TABLE 3

DIMENSIONS OF ANGLE SPECIMENS

Specimen	Length 2L(in.)	Width b(in.)	Thickness t (in.)	b/t	2L/b	Area (in^2)
A-21	25.0	4.87	0.383	12.70	5.14	3.78
A-22	25.0	4.79	0.381	12.60	5.21	3.70
A-31	17.9	3.27	0.370	8.85	5.48	2.48
A-32	17.9	3.28	0.374	8.79	5.46	2.51
A-41	12.5	2.31	0.377	6.13	5.41	1.80
A-42	12.5	2.34	0.371	6.36	5.35	1.81

TABLE 4

RESULTS OF ANGLE TESTS

Test	σ_y ksi	$\epsilon_{cr} \cdot 10^3$	σ_{cr} ksi	Type of Buckling
A-22	---	3.0	32.2	torsional
A-31	34.9	16.5	35.8	torsional
A-32	34.6	16.5	35.6	torsional
A-41	35.3	--	--	bending
A-42	34.1	--	--	bending

TABLE 5

DIMENSIONS OF WF SPECIMENS

Spec.	Shape	A in^2	Z in^3	2b in	t_f in	d in	t_w in	L in	L^1 in	b/t_f	d/t_w
B1 D1	10WF33	9.66	38.56	7.95	0.429	9.37	0.294	32	32	9.2	31.9
B2 D2	8WF24	6.83	22.56	6.55	0.383	7.63	0.236	26	26	8.6	32.3
B3 D3	10WF39	11.34	45.63	8.02	0.512	9.37	0.328	32	32	7.8	28.6
B4 D4	12WF50	14.25	70.28	8.18	0.620	11.57	0.351	32	32	6.6	33.0
B5 D5	8WF35	10.00	33.68	8.08	0.476	7.65	0.308	32	32	8.5	24.8
B6 D6	10WF21	5.84	22.45	5.77	0.318	9.56	0.232	23	26	9.1	40.9

A = area of cross-section

Z = plastic section modulus (twice the static moment of half the section about the strong axis)

2b = width of flange

t_f = thickness of flange

d = distance between center planes of flanges

t_w = thickness of web

L = length of compression specimen

L^1 = length of part of bending specimen subjected to pure bending

TABLE 6

RESULTS OF WF TESTS

Test	σ_y ksi	$\epsilon_{cr} \cdot 10^3$		σ_{cr} ksi		Type of Buckling
		Flange	Web	Flange	Web	
D 1	34.4	8.5	8.5	34.2	34.2	flange
D 2	34.0	13.5	12.7	34.0	34.0	flange & web
D 3	35.2	19.0	19.0	39.0	39.0	flange
D 4	35.0	18.5	5.0	36.8	35.4	web
D 5	36.6	17.0	17.0	38.0	38.0	flange
D 6	38.0	4.3	1.6	33.8	37.2	web
B 1	-	7.0	-	-	-	flange
B 2	-	23.0	-	-	-	flange & lateral
B 3	-	22.5	-	-	-	flange & lateral
B 4	-	29.0	-	-	-	lateral
B 5	-	22.0	-	-	-	flange & lateral
B 6	-	14.0	-	-	-	flange & lateral

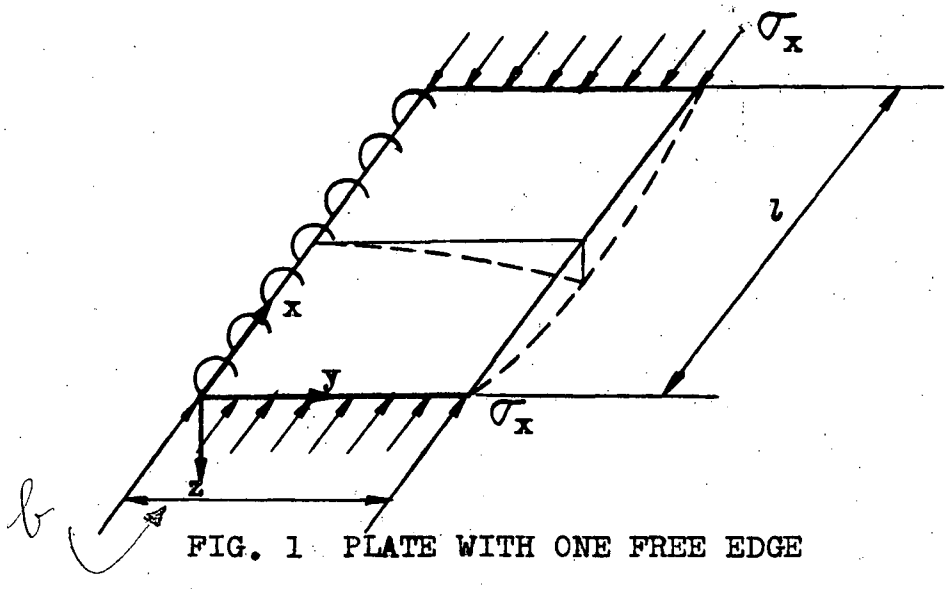

FIG. 1 PLATE WITH ONE FREE EDGE

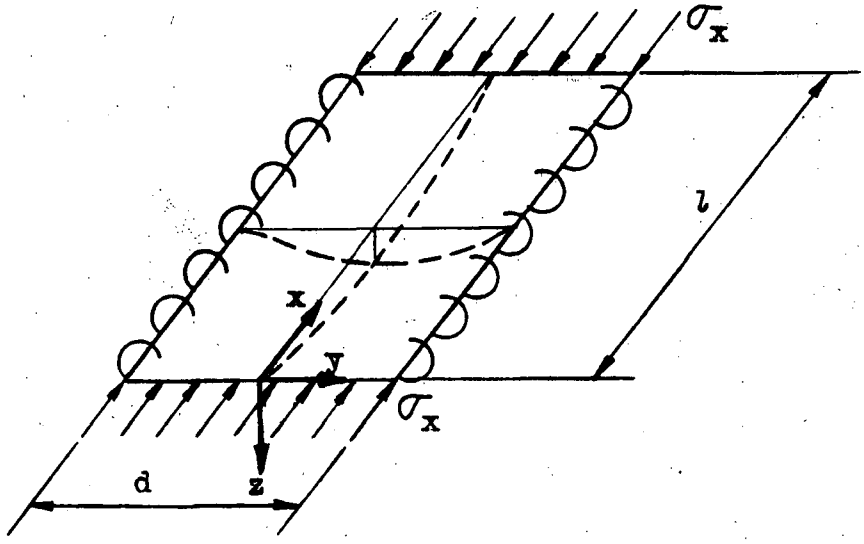

FIG. 2 PLATE SUPPORTED AT ALL FOUR EDGES

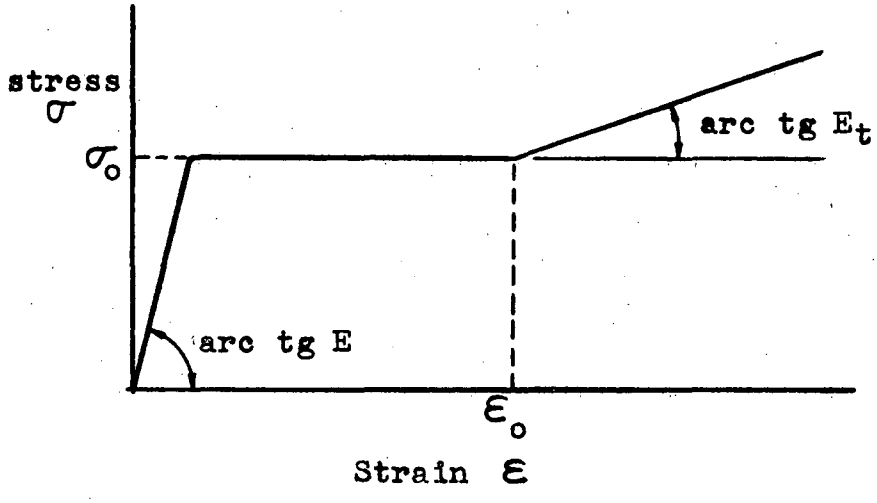

FIG. 3 SIMPLIFIED STRESS-STRAIN CURVE

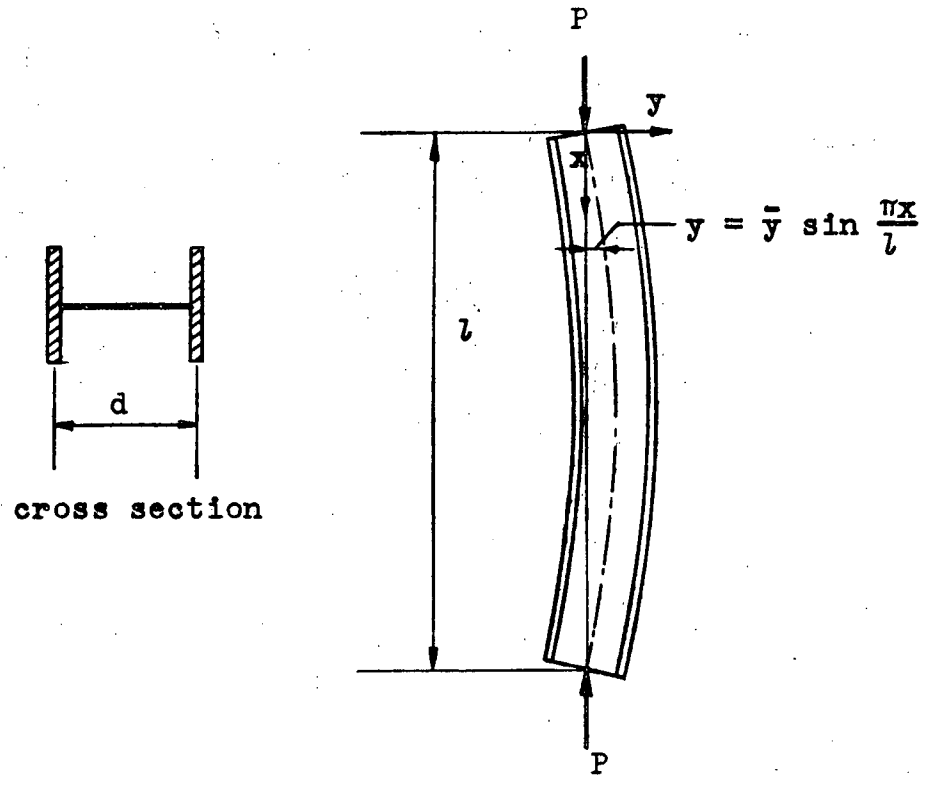

FIG. 4 SIMPLIFIED WF COLUMN

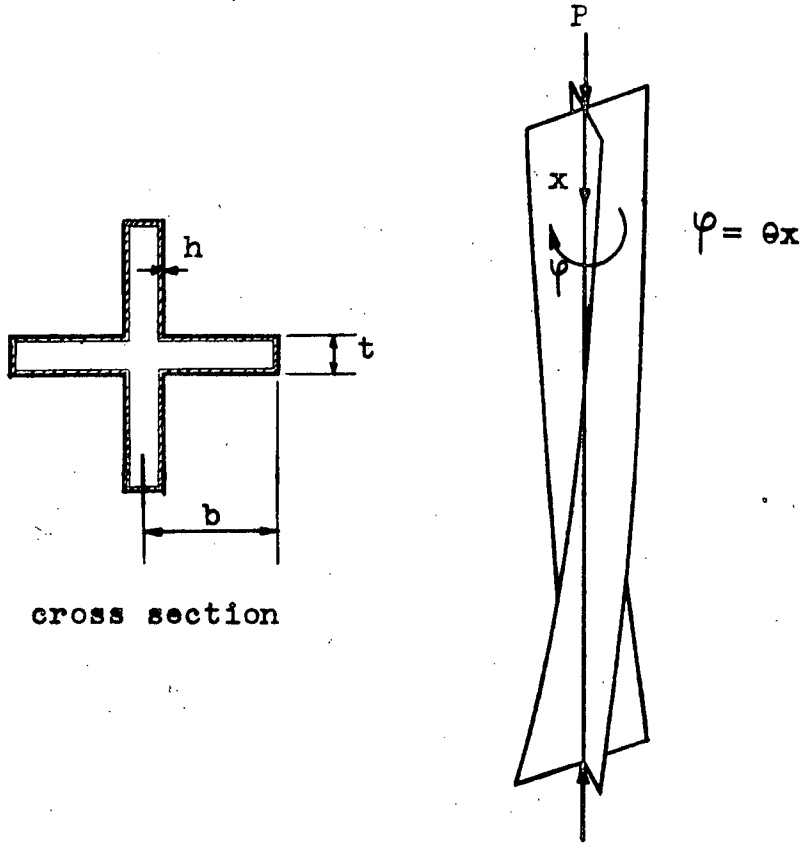

FIG. 5 SIMPLIFIED CRUCIFORM COLUMN

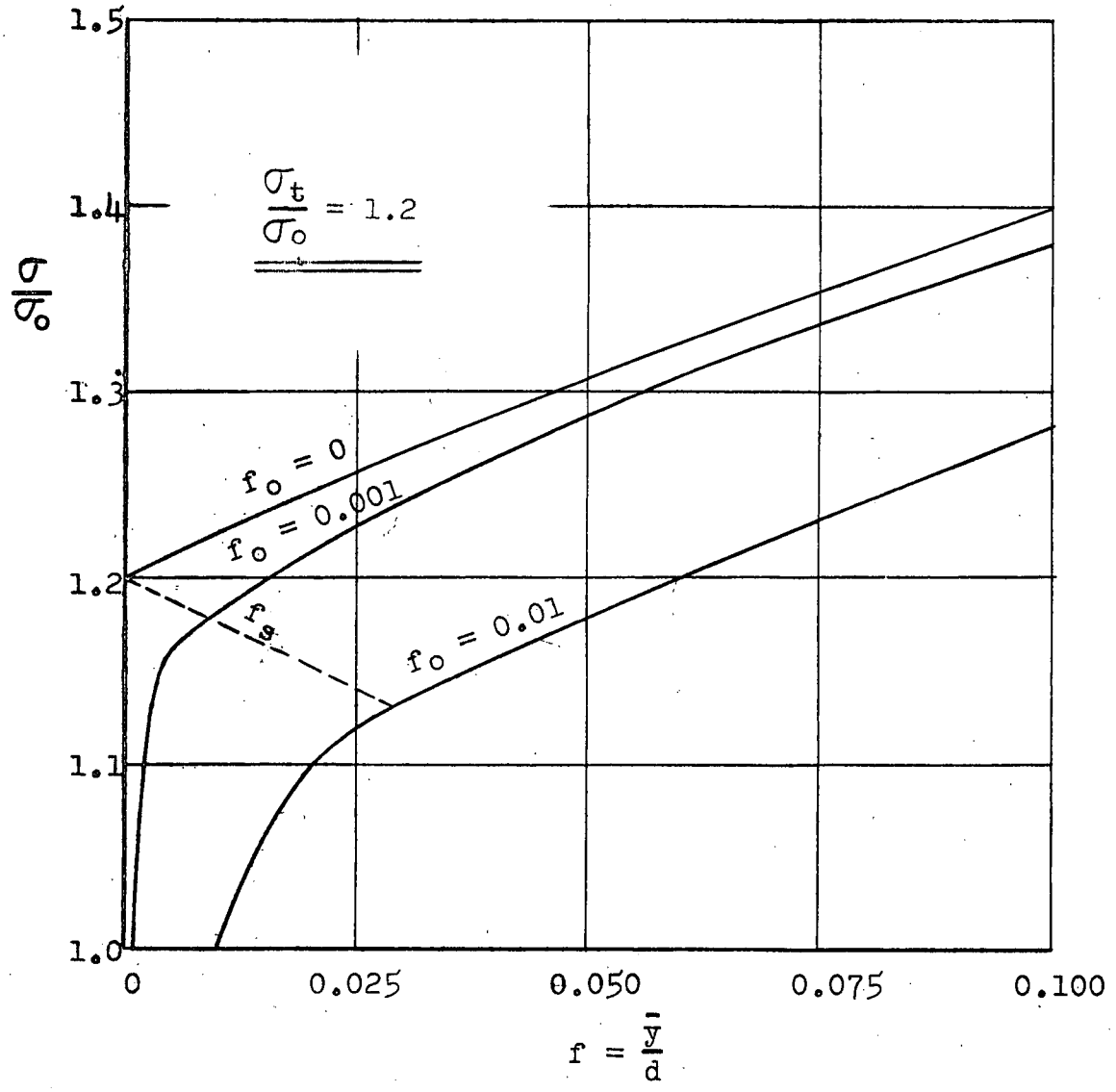

FIG. 6 EFFECT OF INITIAL IMPERFECTIONS ON A SIMPLIFIED WF SECTION

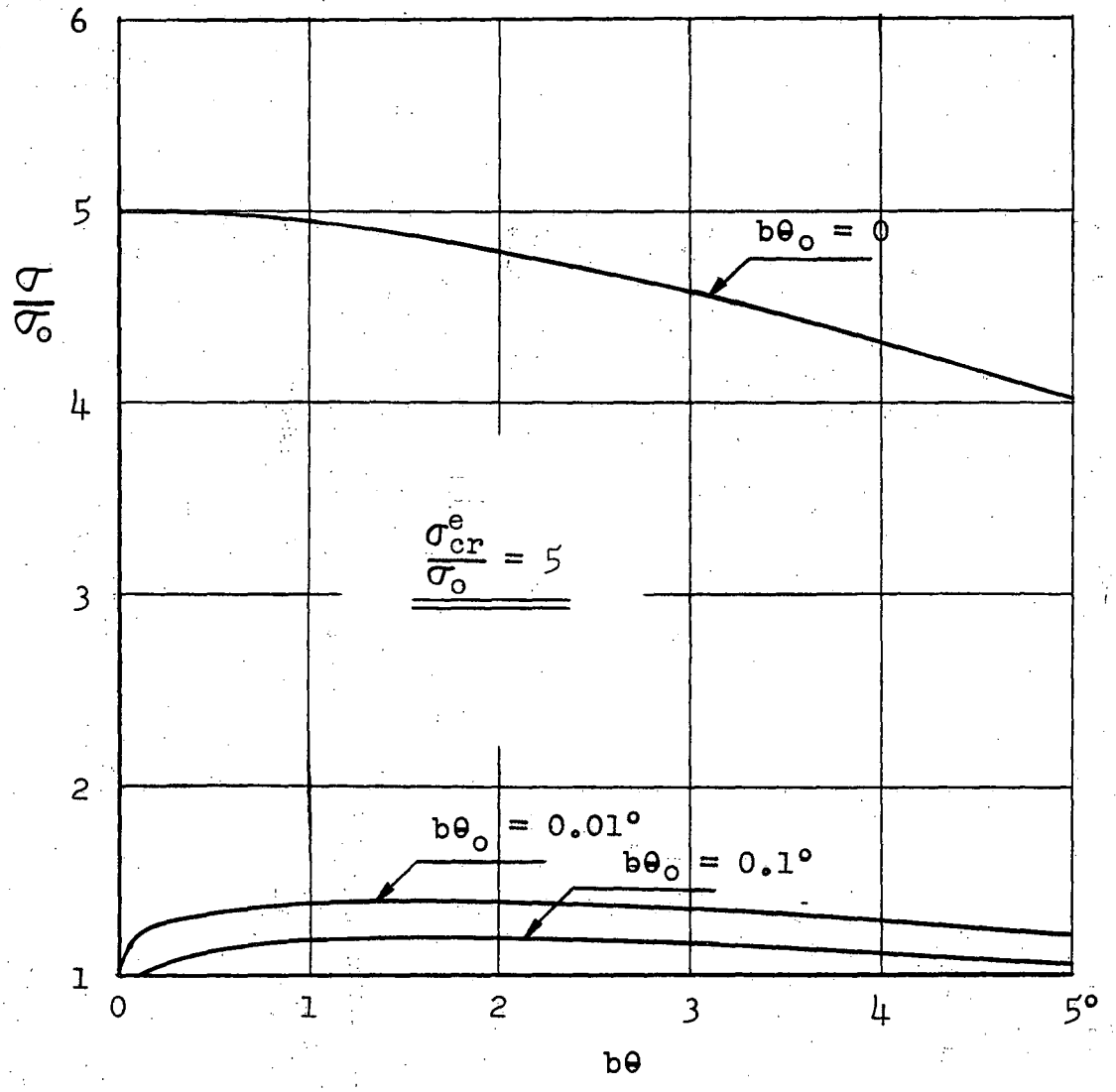

FIG. 7 INFLUENCE OF INITIAL IMPERFECTIONS ON A SIMPLIFIED CRUCIFORM SECTION

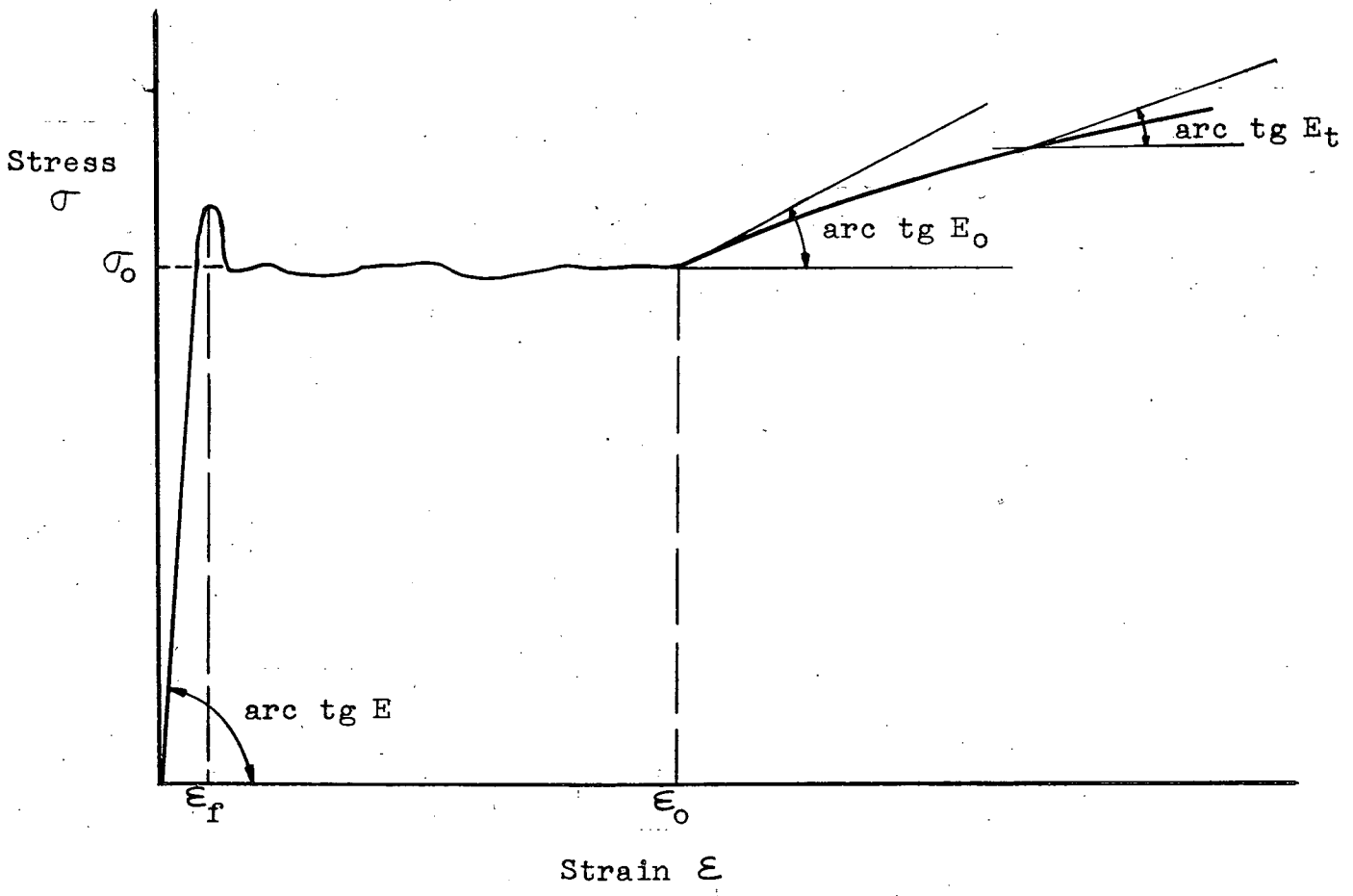

FIG. 8 TYPICAL STRESS-STRAIN CURVE OBTAINED FROM COUPON TEST

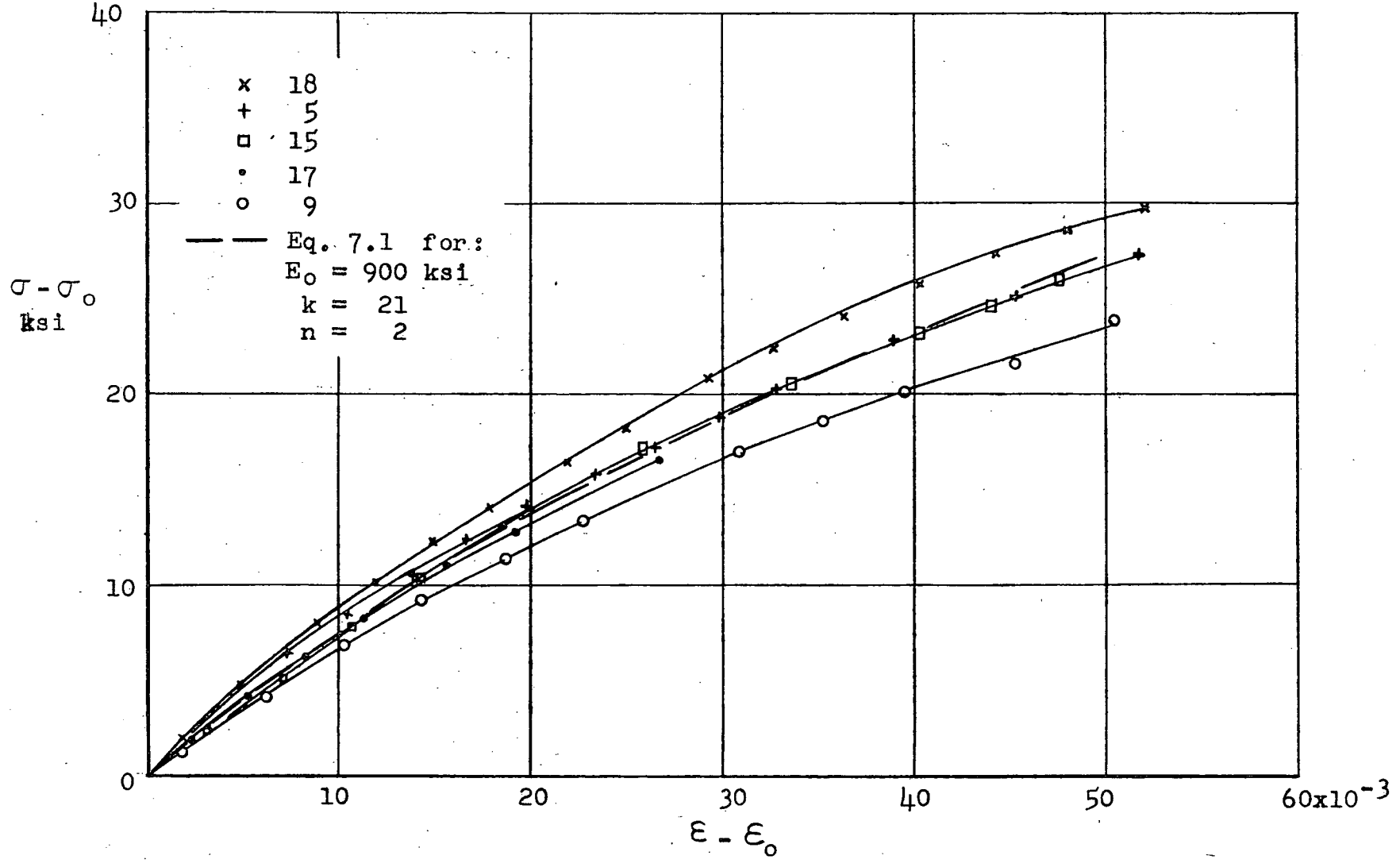

FIG. 9 RESULTS OF COMPRESSION COUPON TESTS

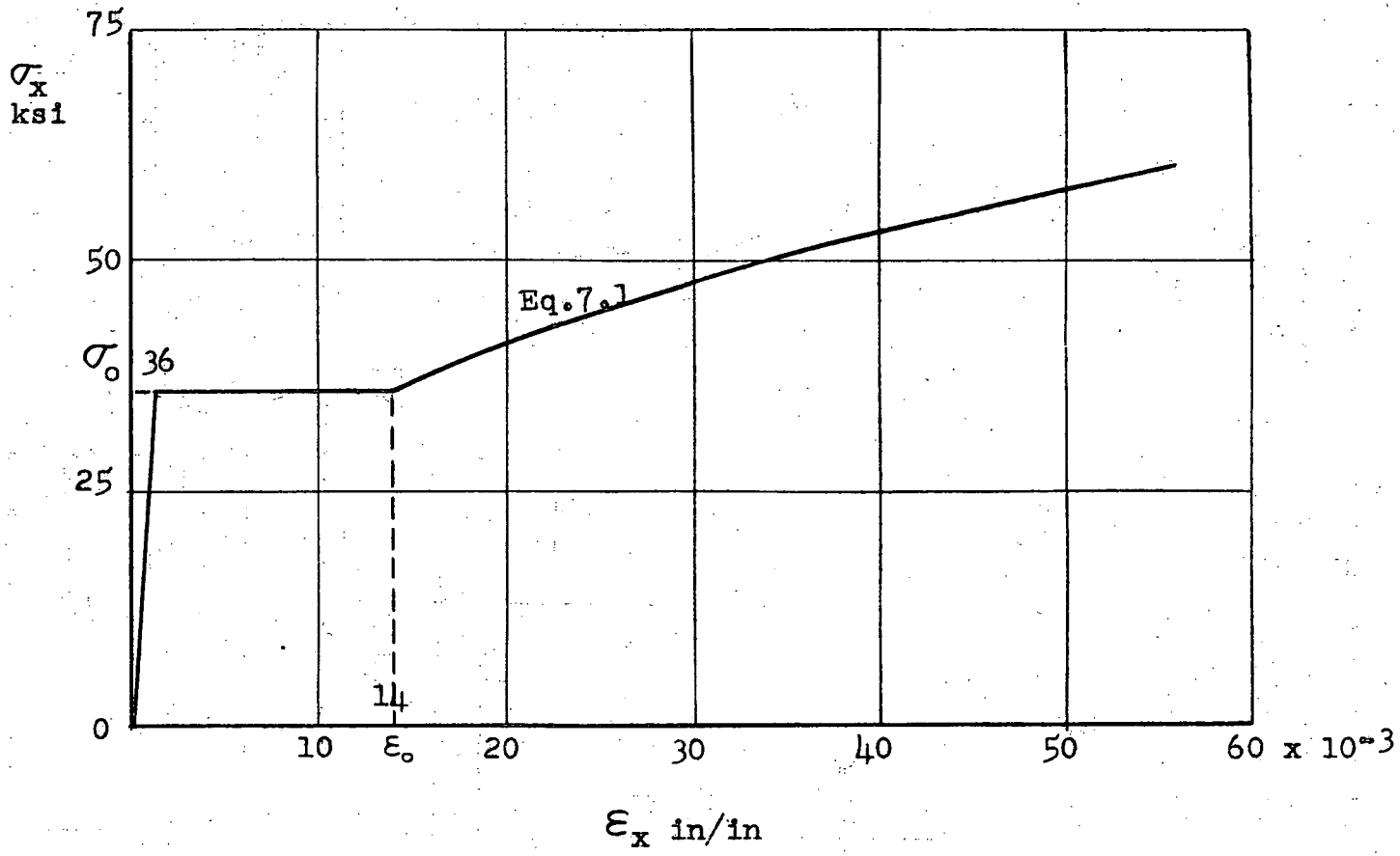

FIG. 10 STRESS-STRAIN CURVE FOR UNI-AXIAL COMPRESSION

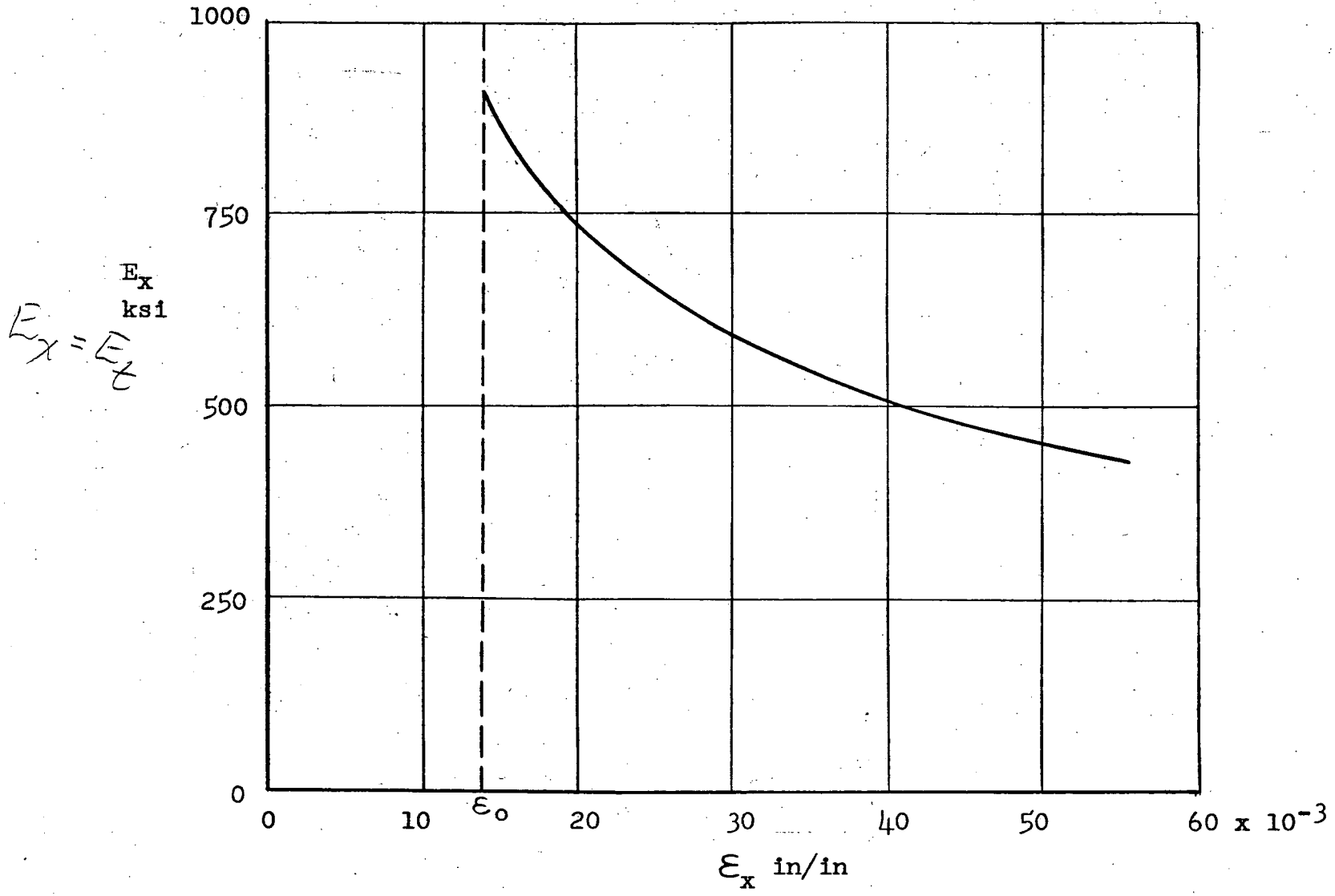

FIG. 11 THE TANGENT-MODULUS IN THE DIRECTION OF LOADING

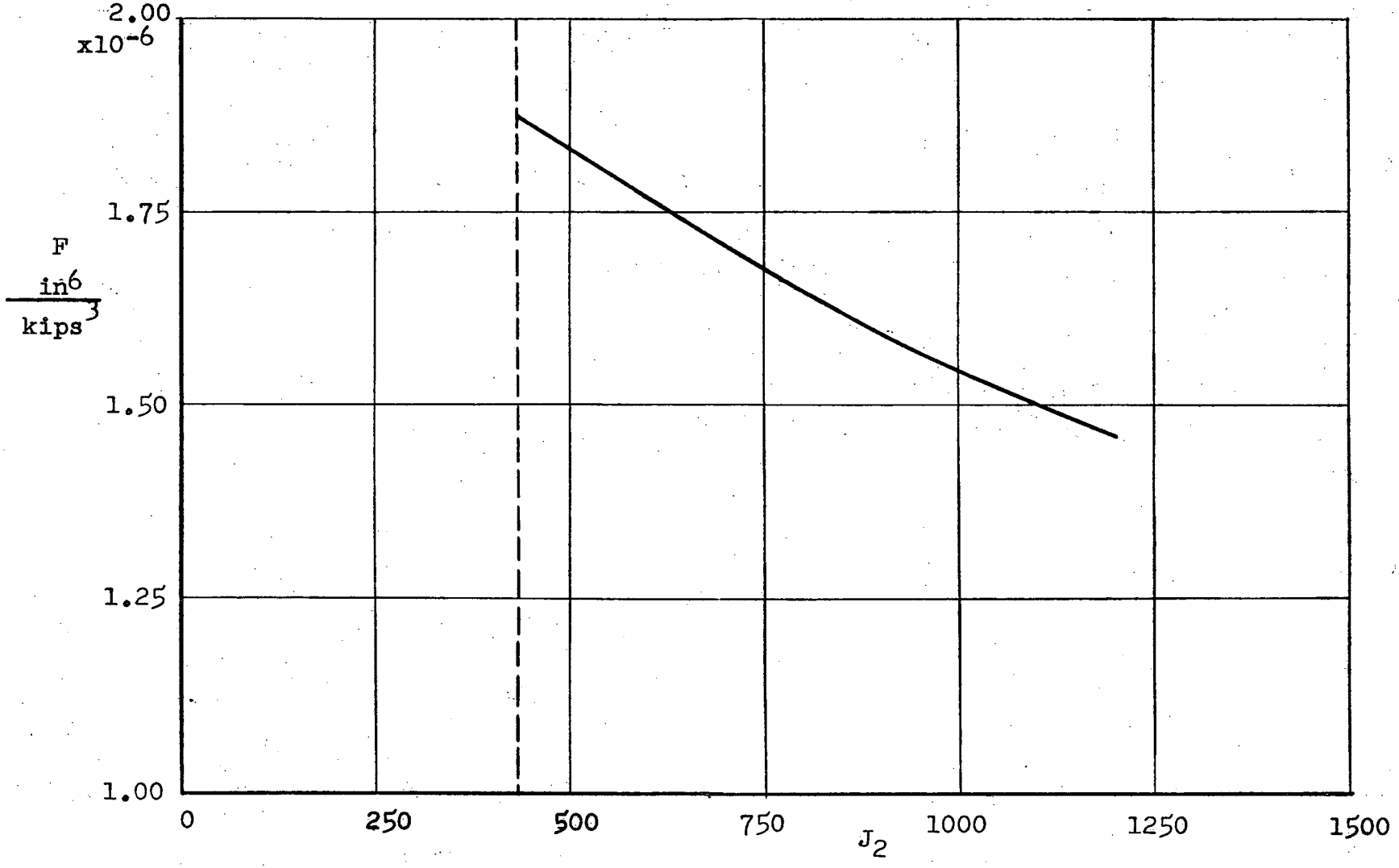

FIG. 12 FUNCTION F(J_2)

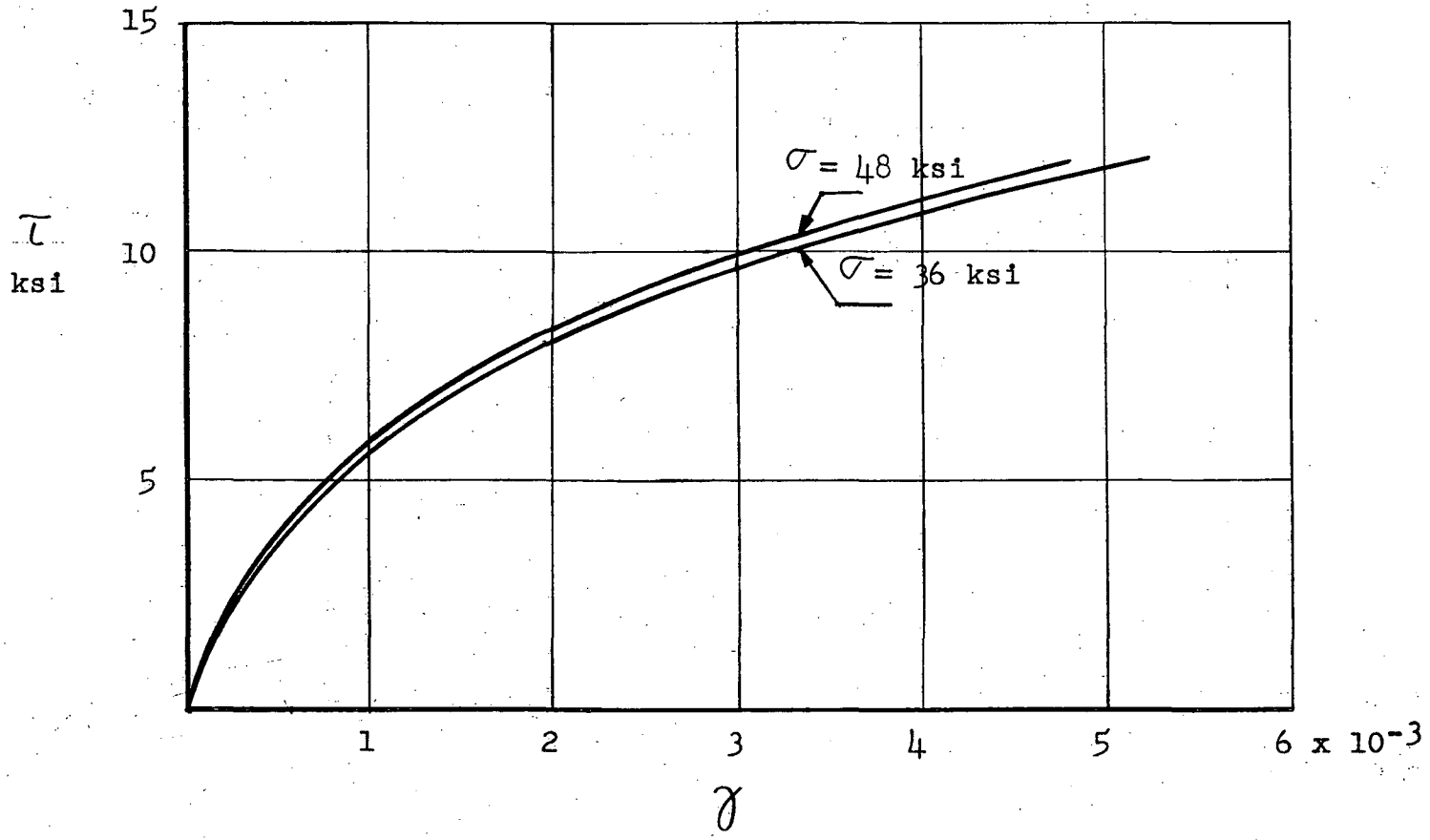

FIG. 13 SUPERPOSITION OF SHEAR STRESS ON CONSTANT NORMAL STRESS

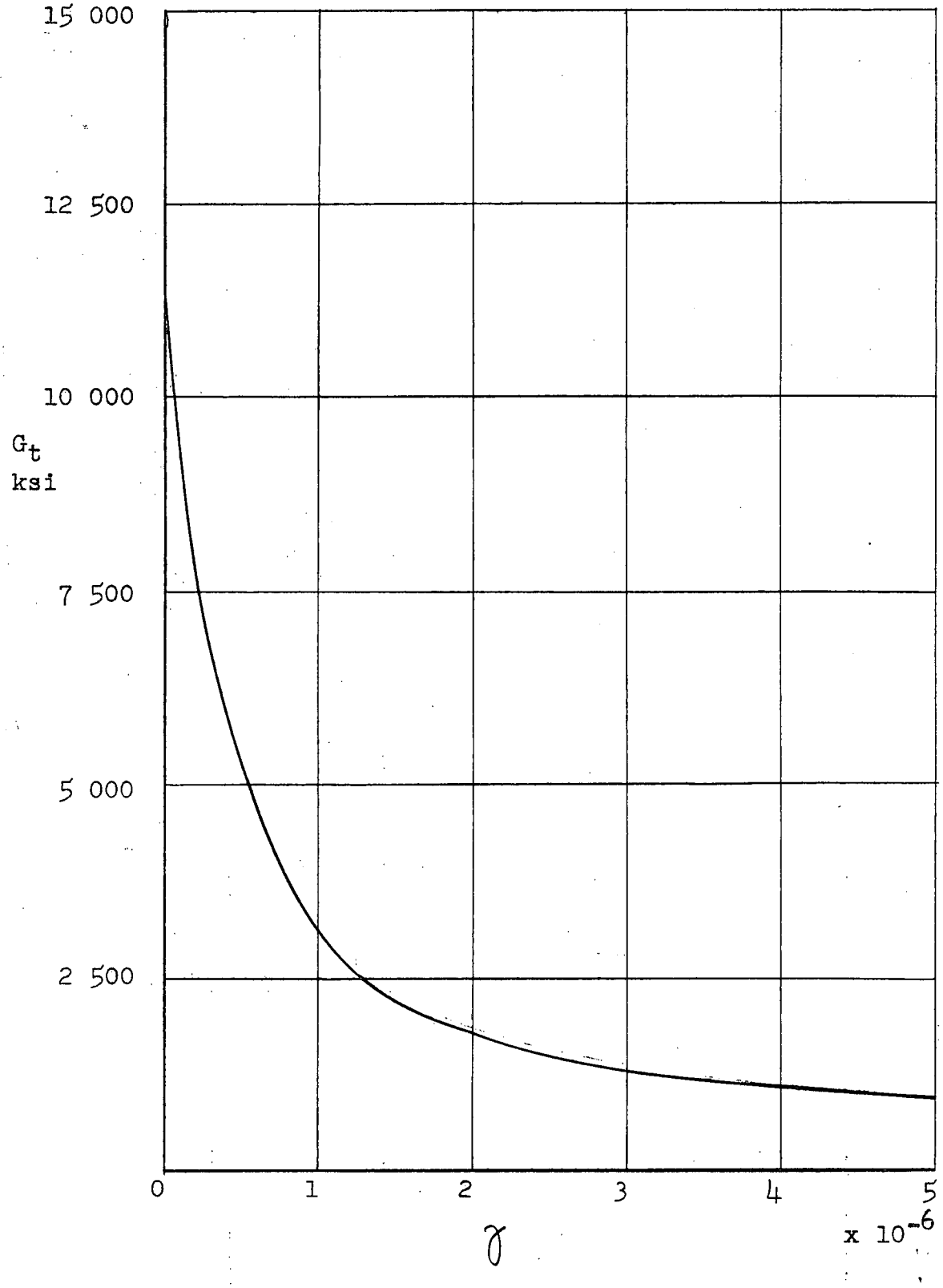

FIG. 14 THE TANGENT SHEAR MODULUS

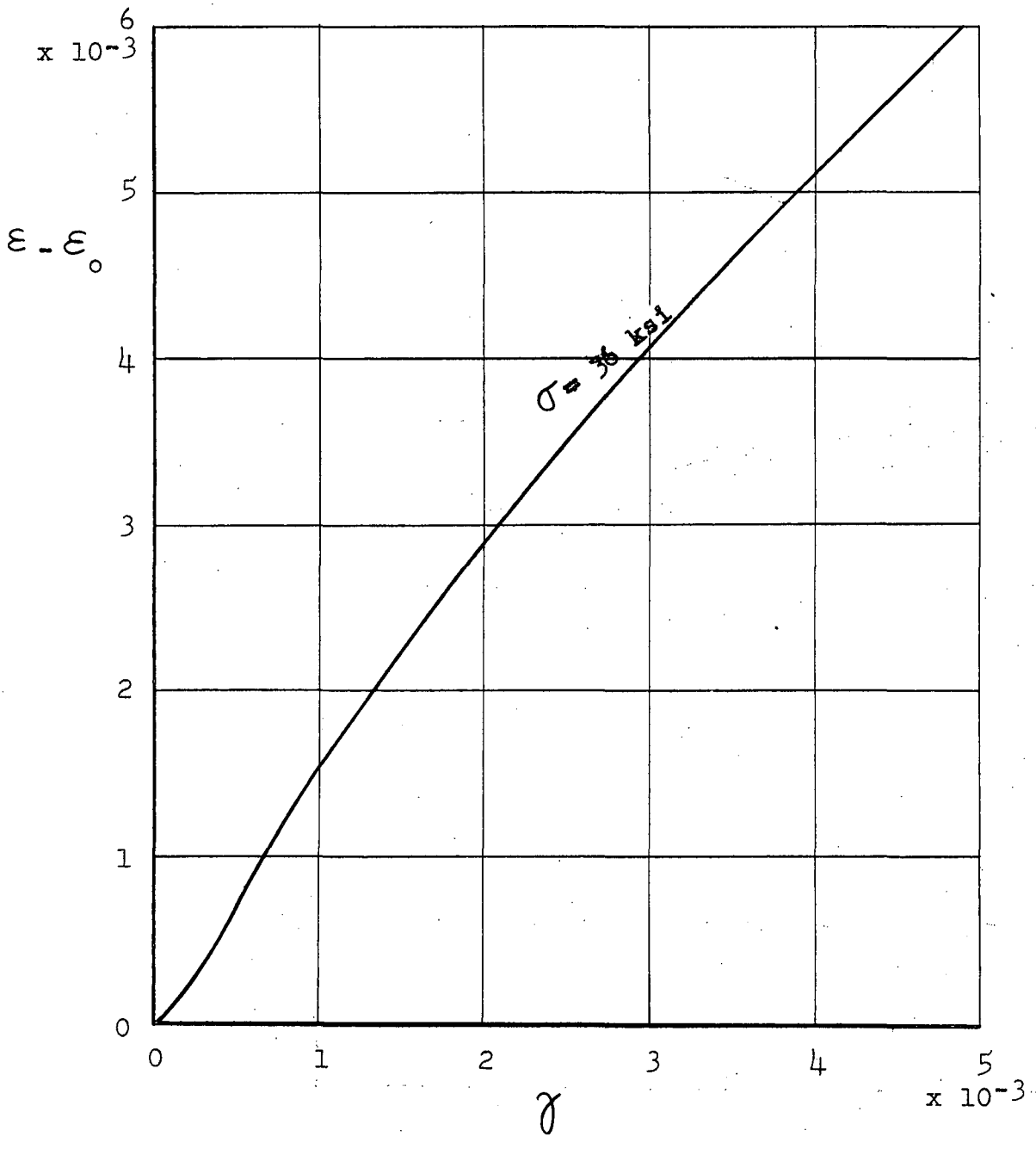

FIG. 15 INCREASE OF AXIAL STRAIN CAUSED BY SHEAR STRESS

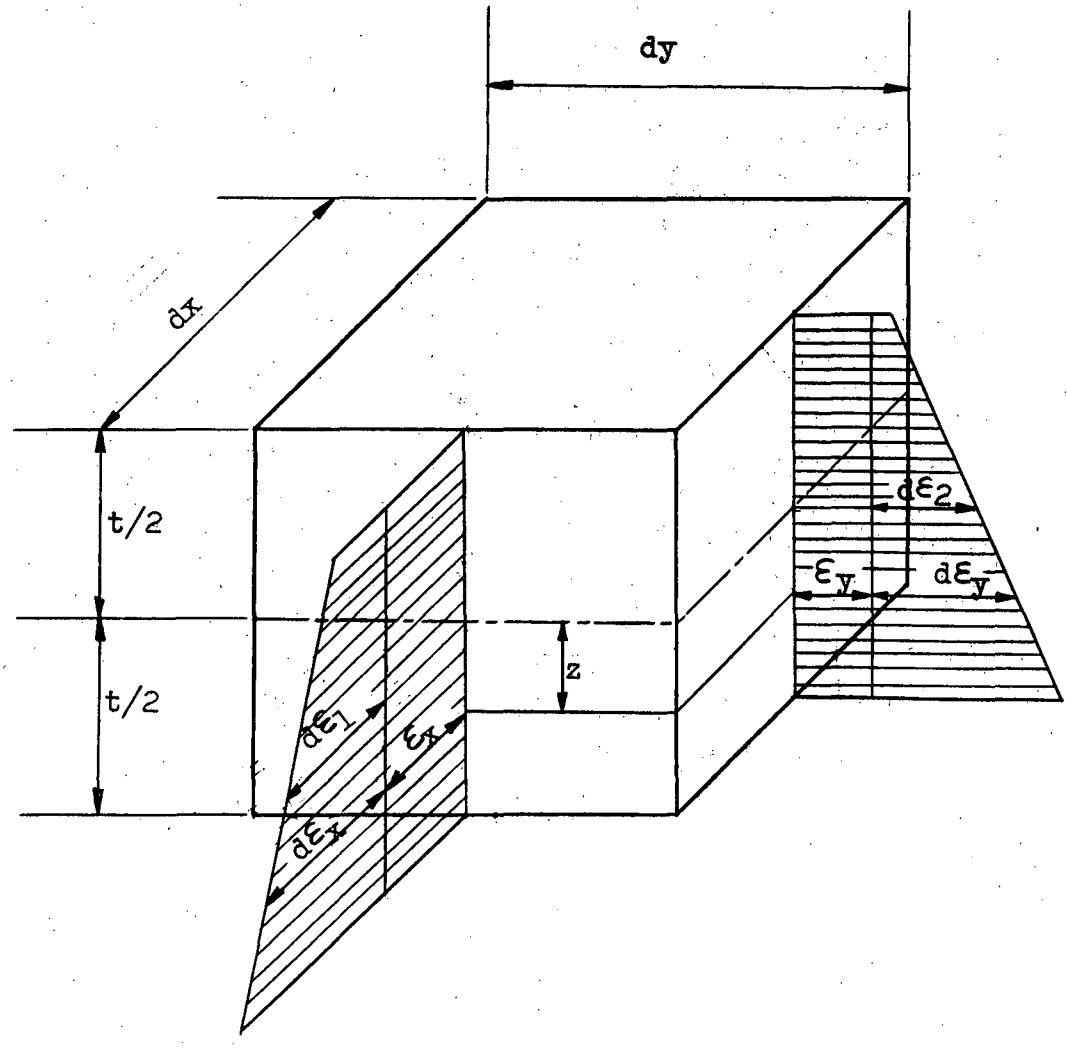

FIG. 16 ASSUMED LINEAR STRAIN DISTRIBUTION

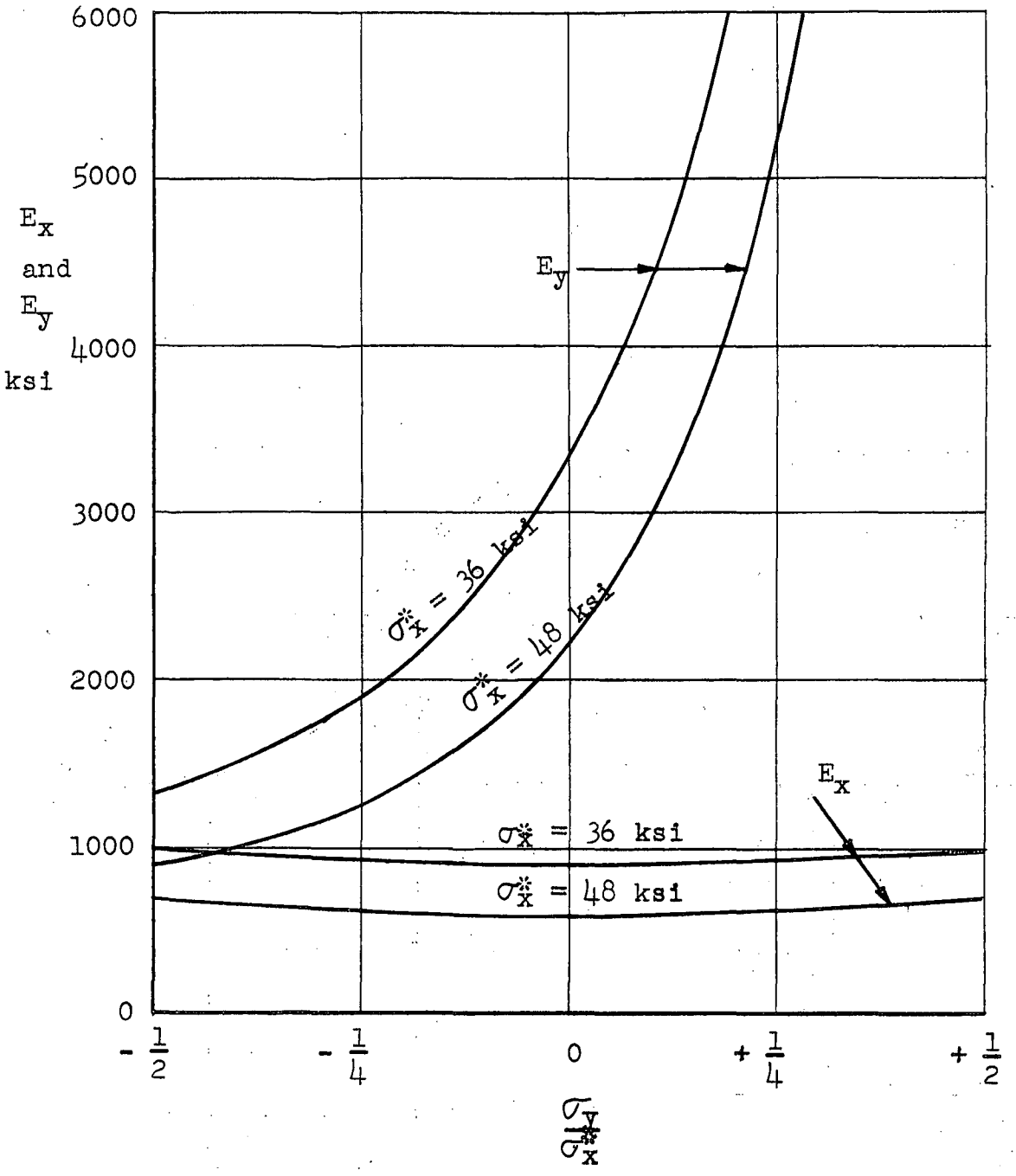

FIG. 17 INFLUENCE OF $\frac{\sigma_y}{\sigma_x^*}$ ON E_x AND E_y

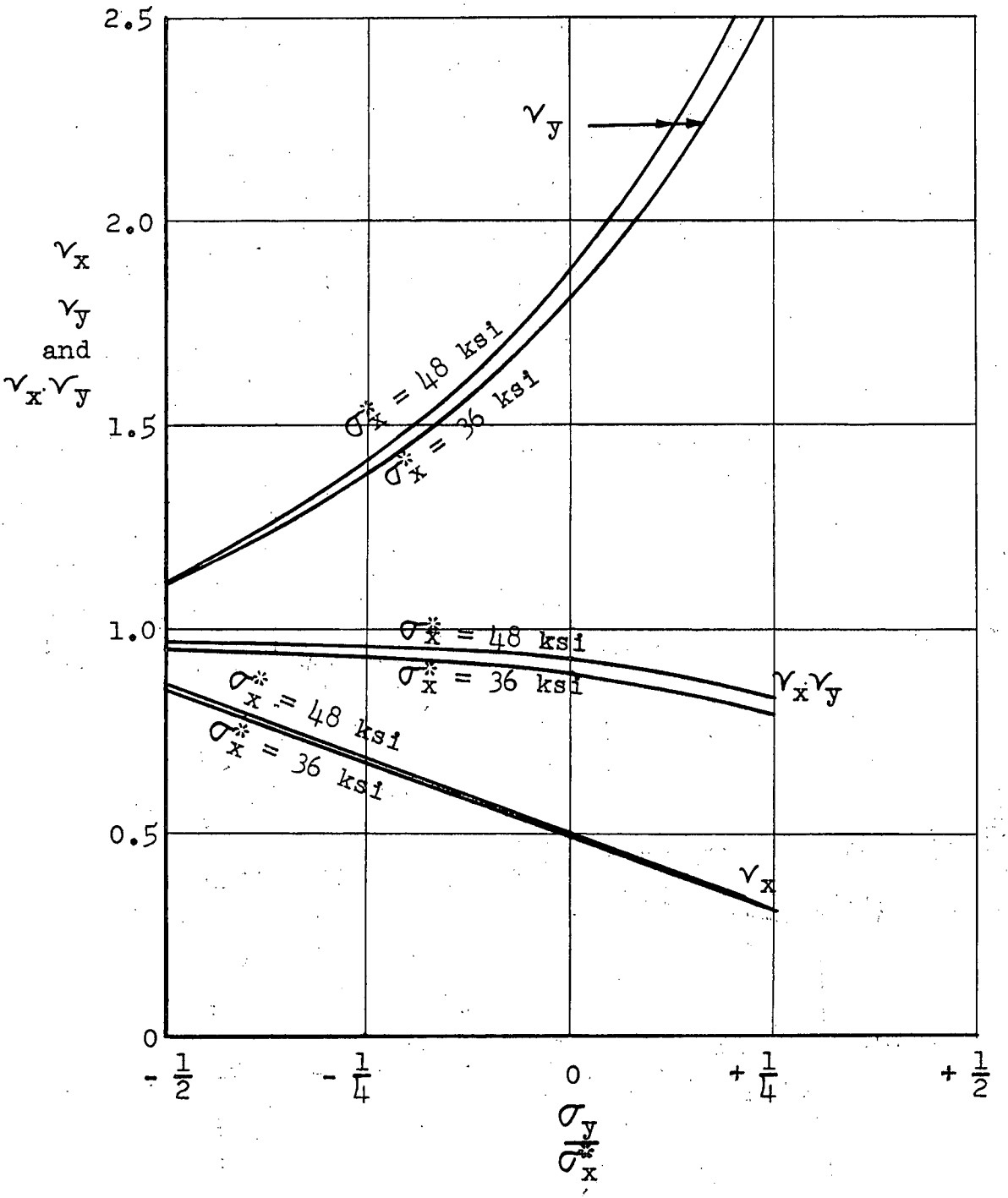

FIG. 18 INFLUENCE OF $\frac{\sigma_y}{\sigma_x^*}$ ON ν_x, ν_y AND $\nu_x \nu_y$

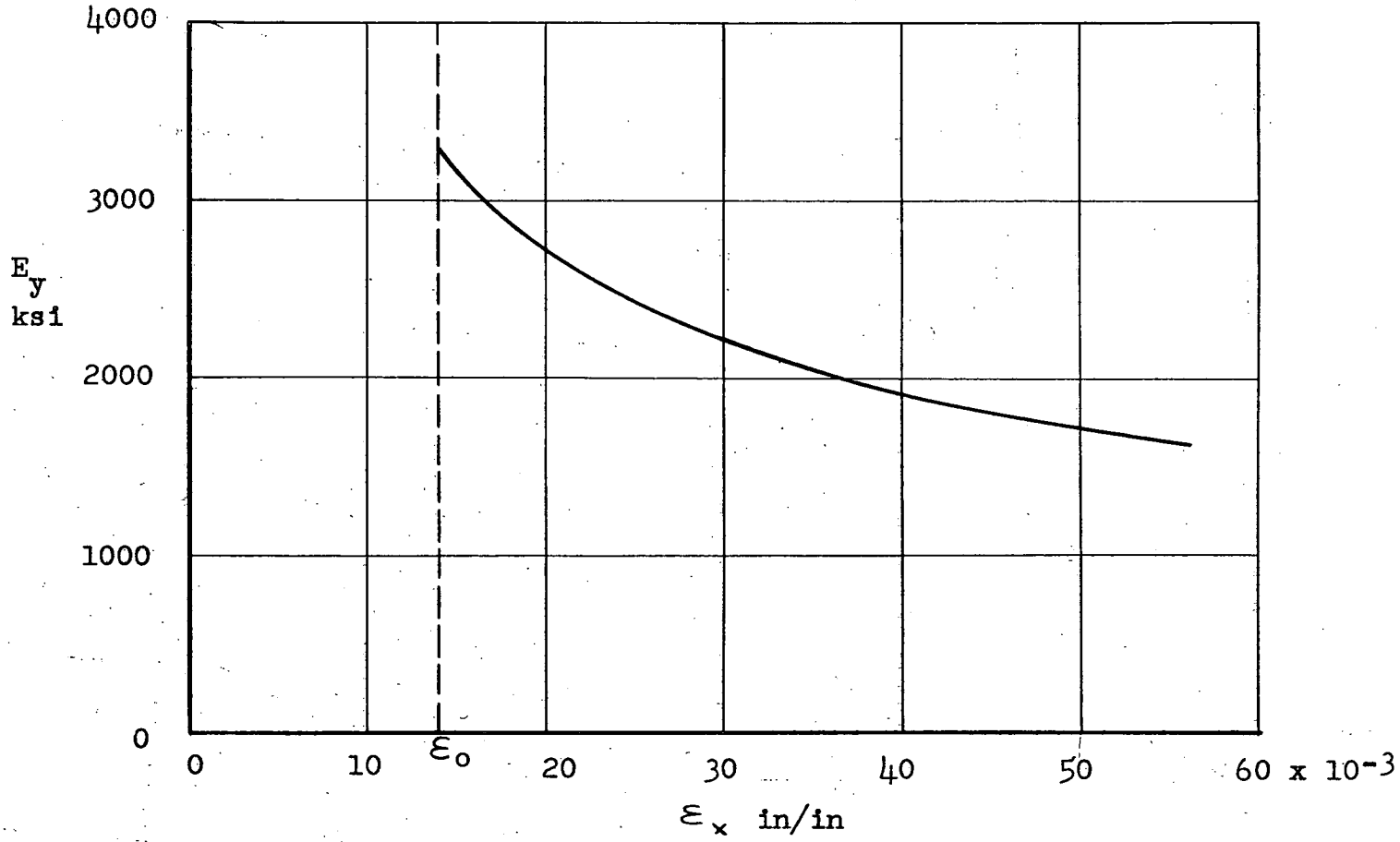

FIG. 19 THE TANGENT MODULUS IN THE Y-DIRECTION

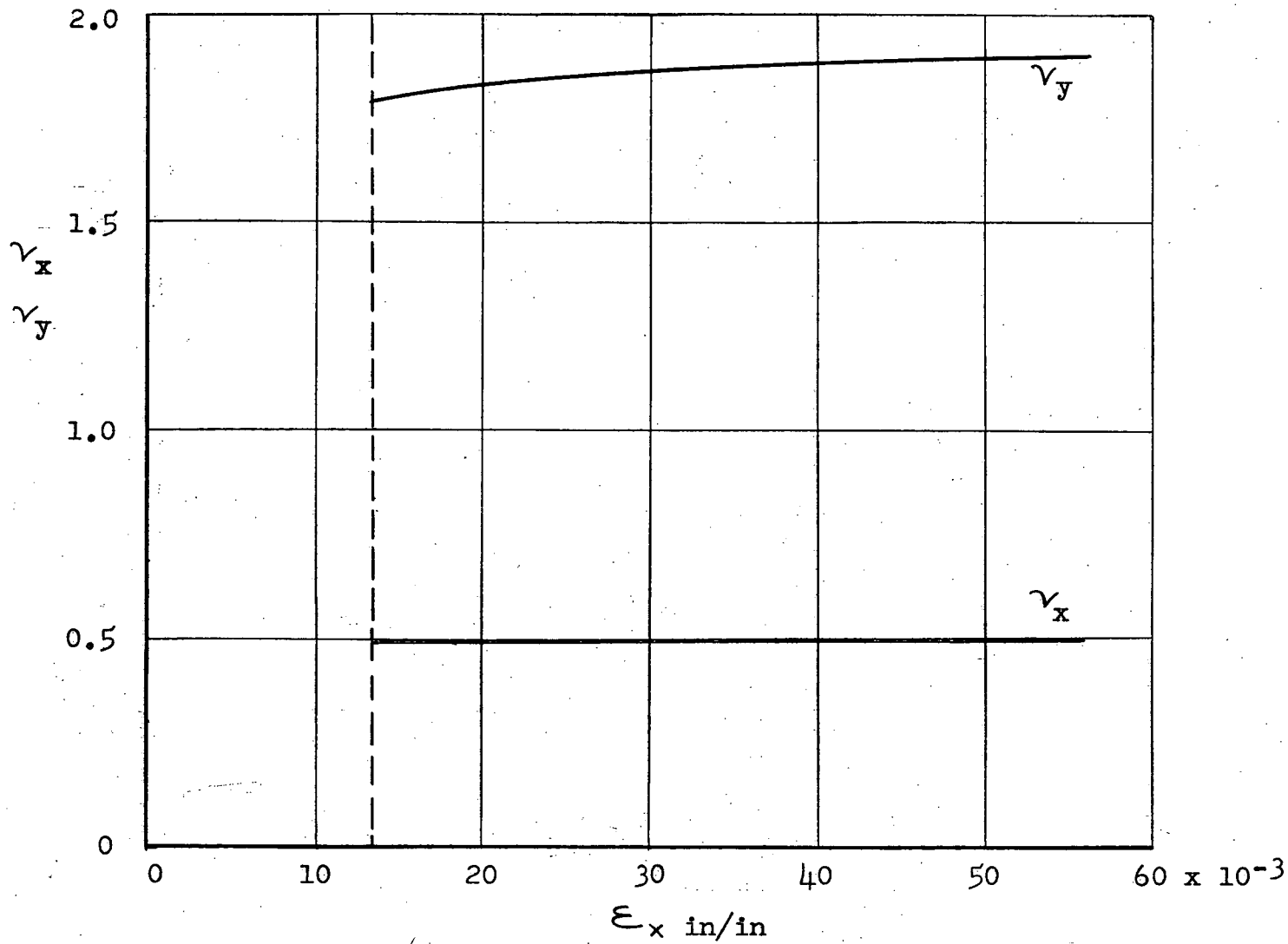

FIG. 20 COEFFICIENTS OF DILATATION ν_x and ν_y

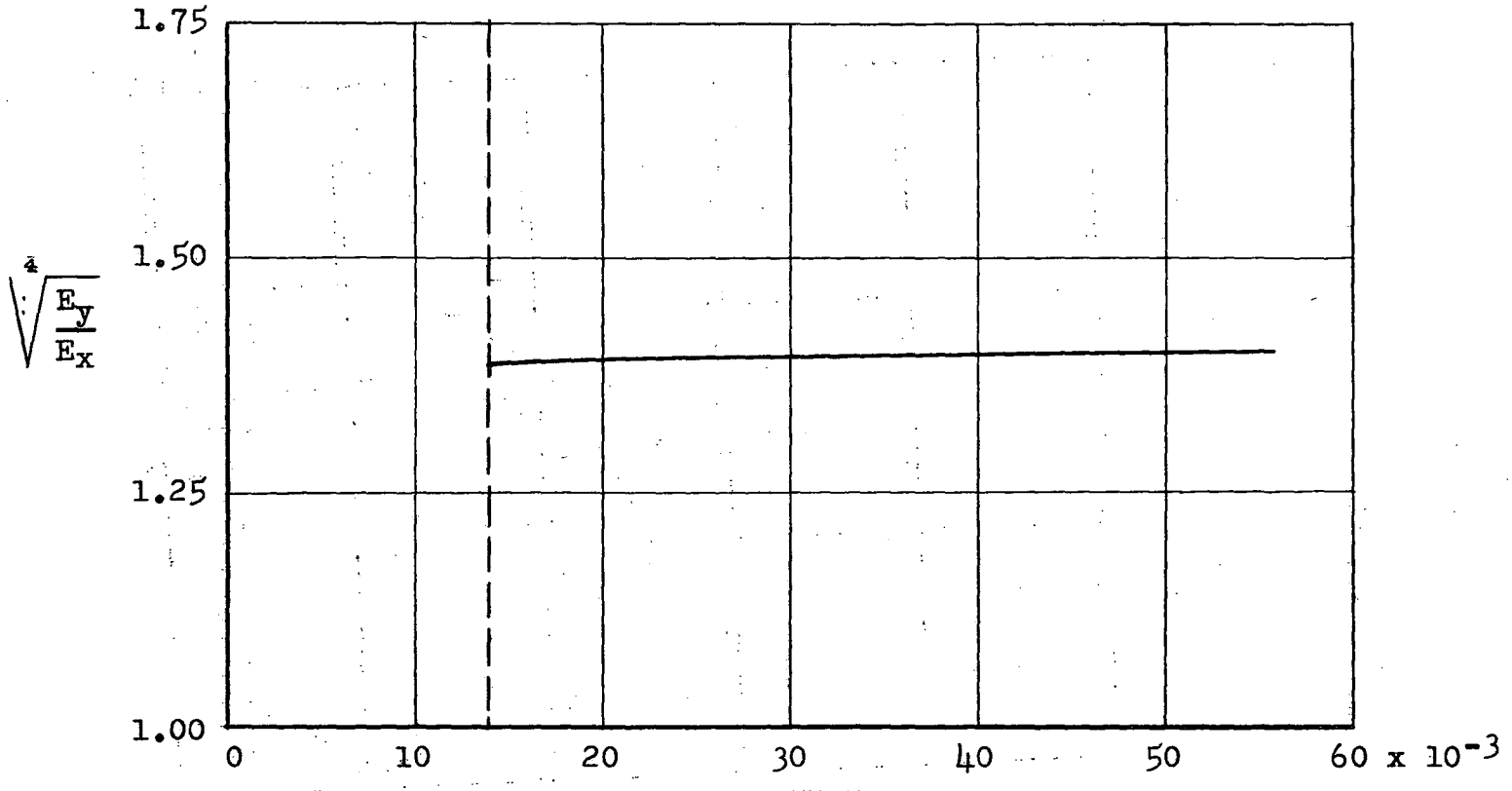

FIG. 21 VARIATION OF $\sqrt[4]{\frac{E_y}{E_x}}$

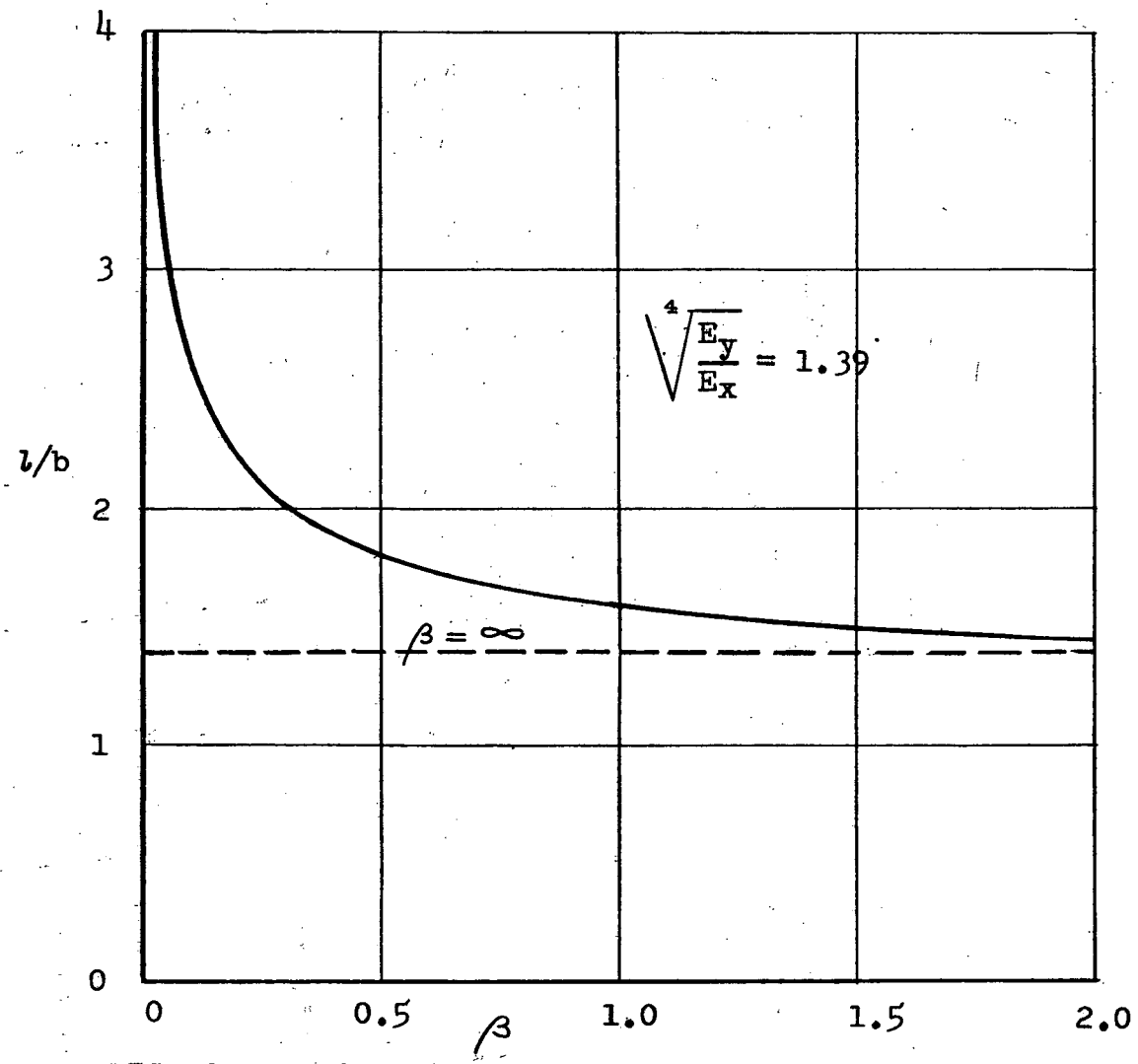

FIG. 22 HALF-WAVE LENGTH OF OUTSTANDING FLANGES

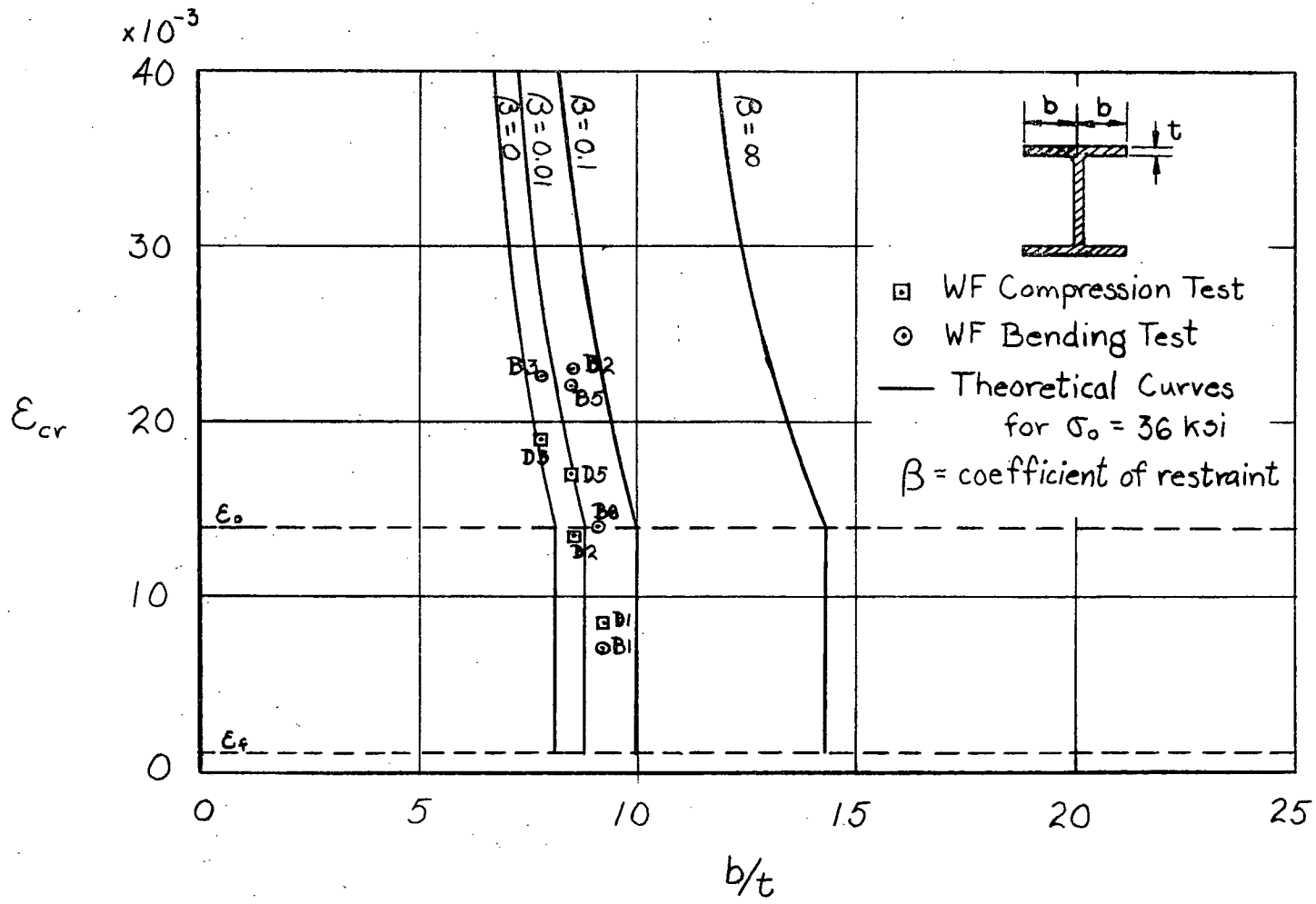

23

Fig. ~~16~~ - Buckling of Wide - Flange Shapes

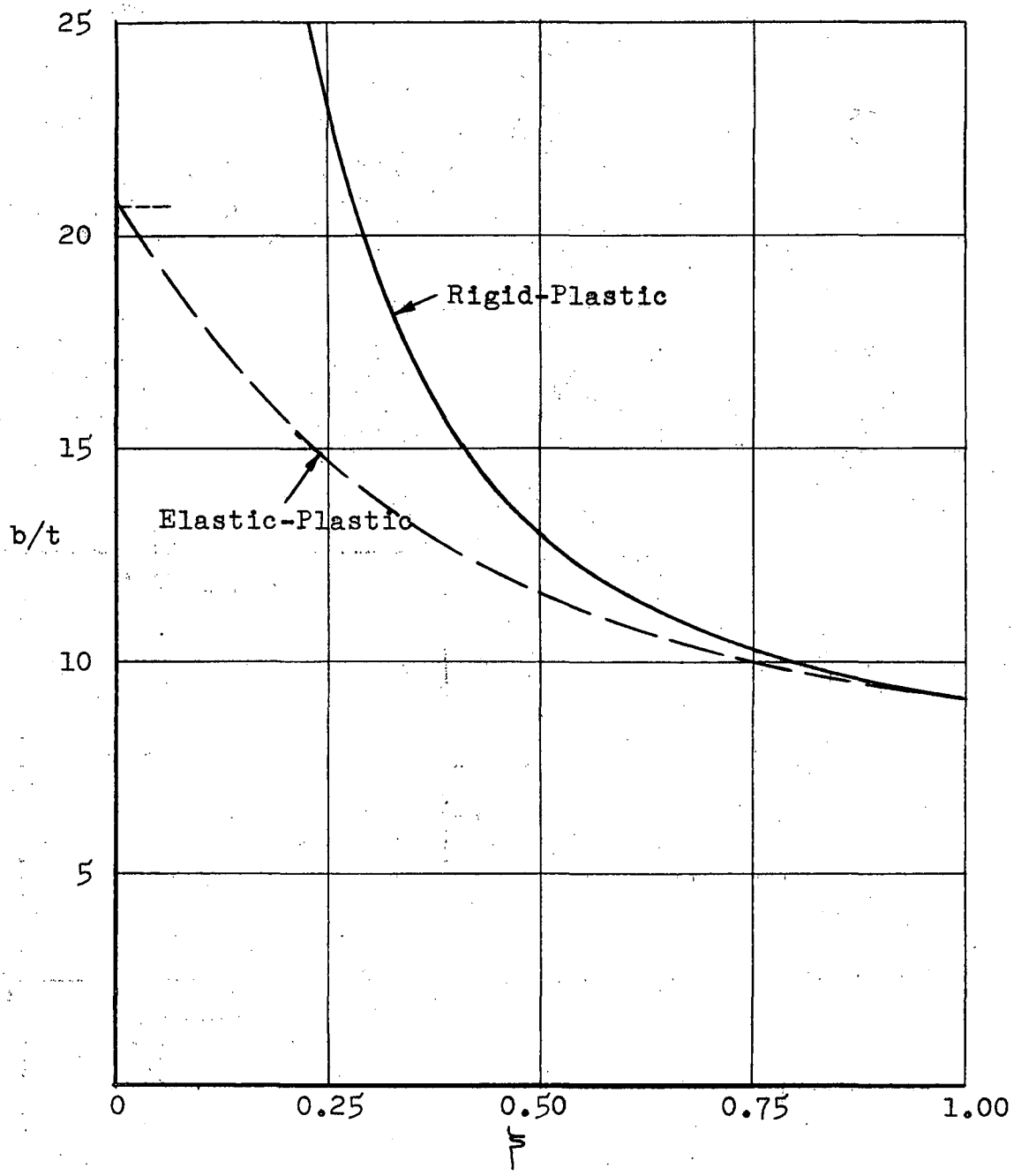

FIG. 24 YIELD PENETRATION $\bar{\delta}$ AS A FUNCTION OF b/t for L/b = 2.65

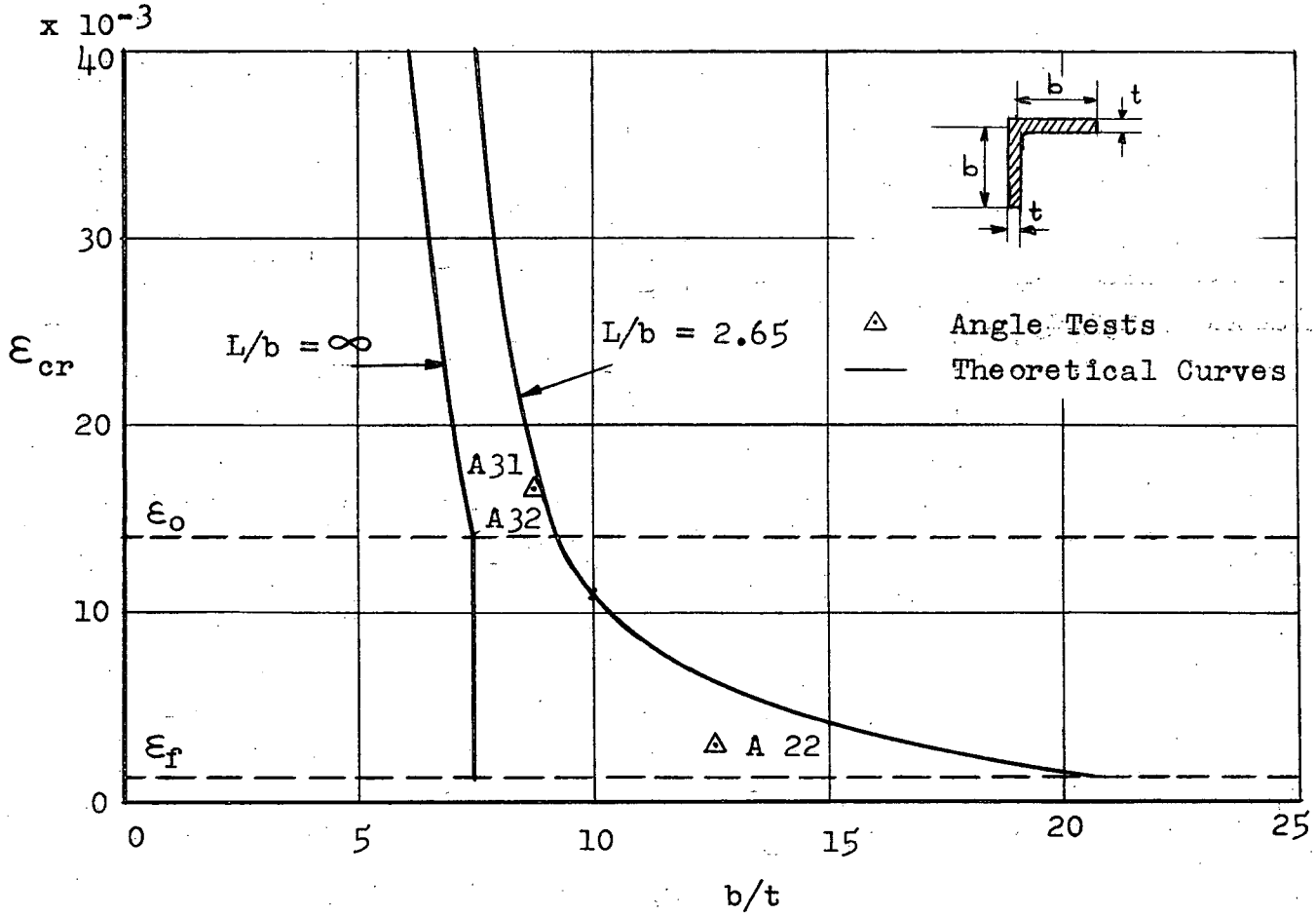

FIG. 25 BUCKLING OF A HINGED FLANGE (Comparison with results of angle tests)

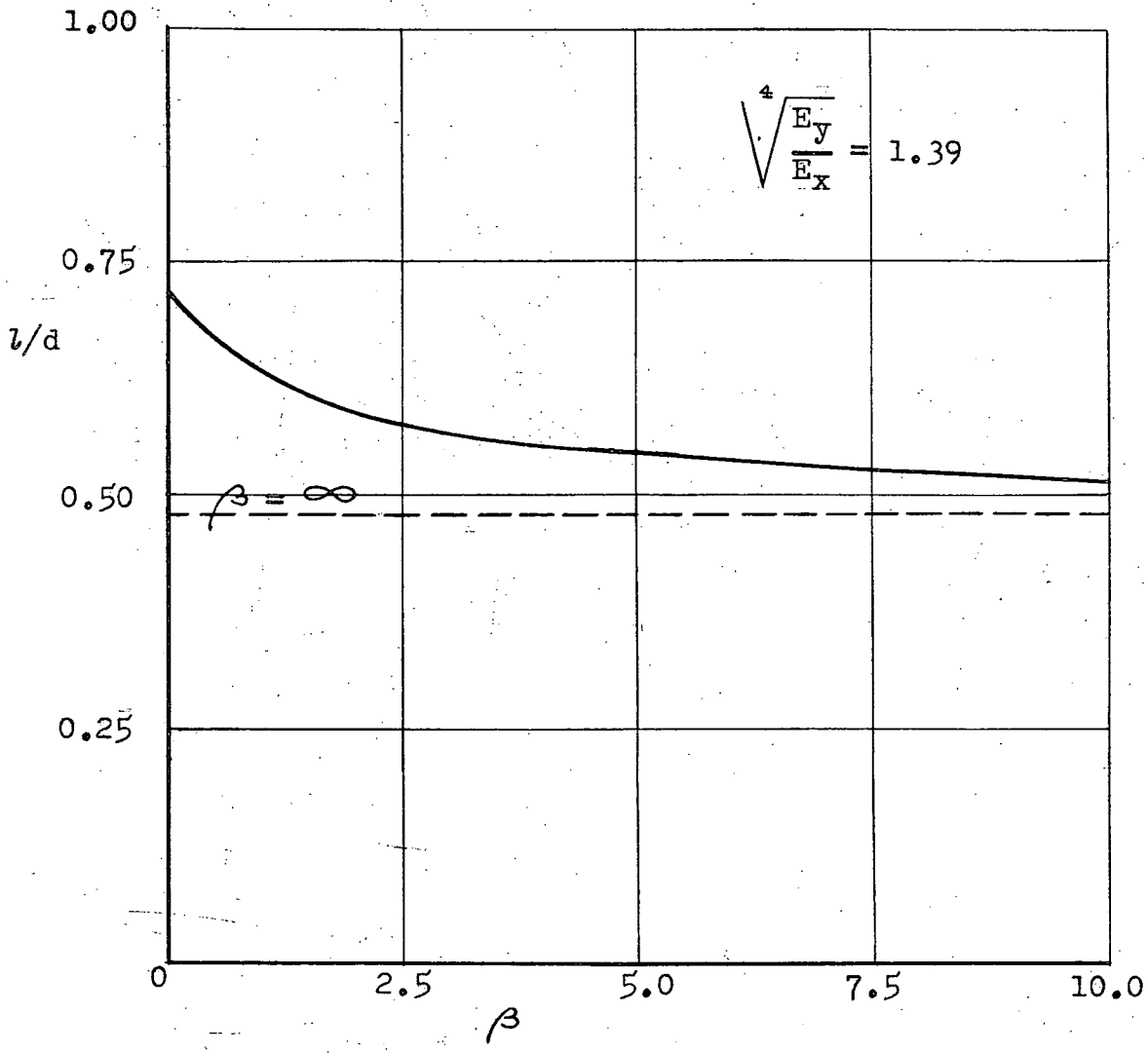

FIG. 26 HAL-WAVE LENGTH OF WEBS

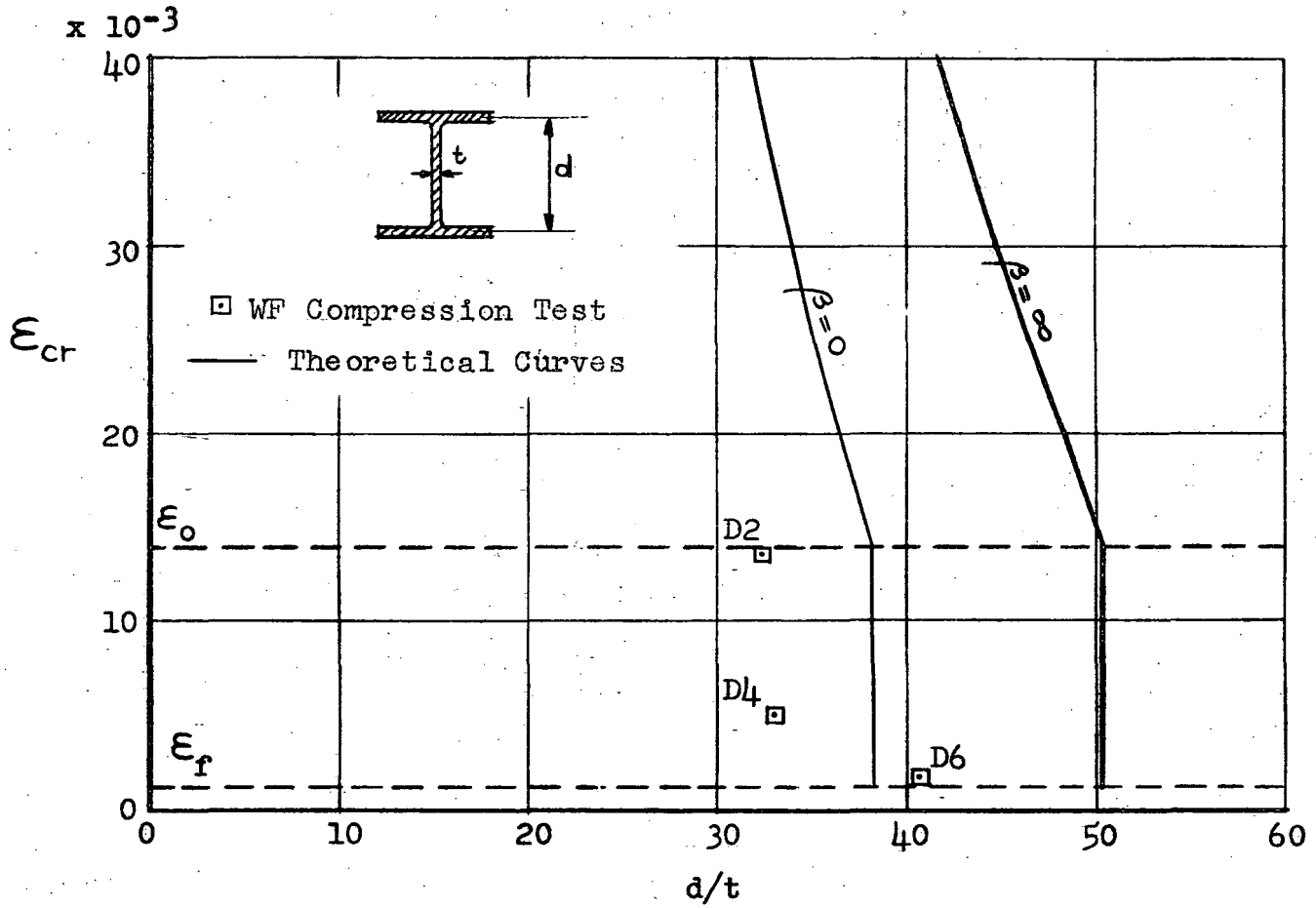

FIG. 27 BUCKLING OF WEBS (Comparison With Results Of WF Compression Tests)

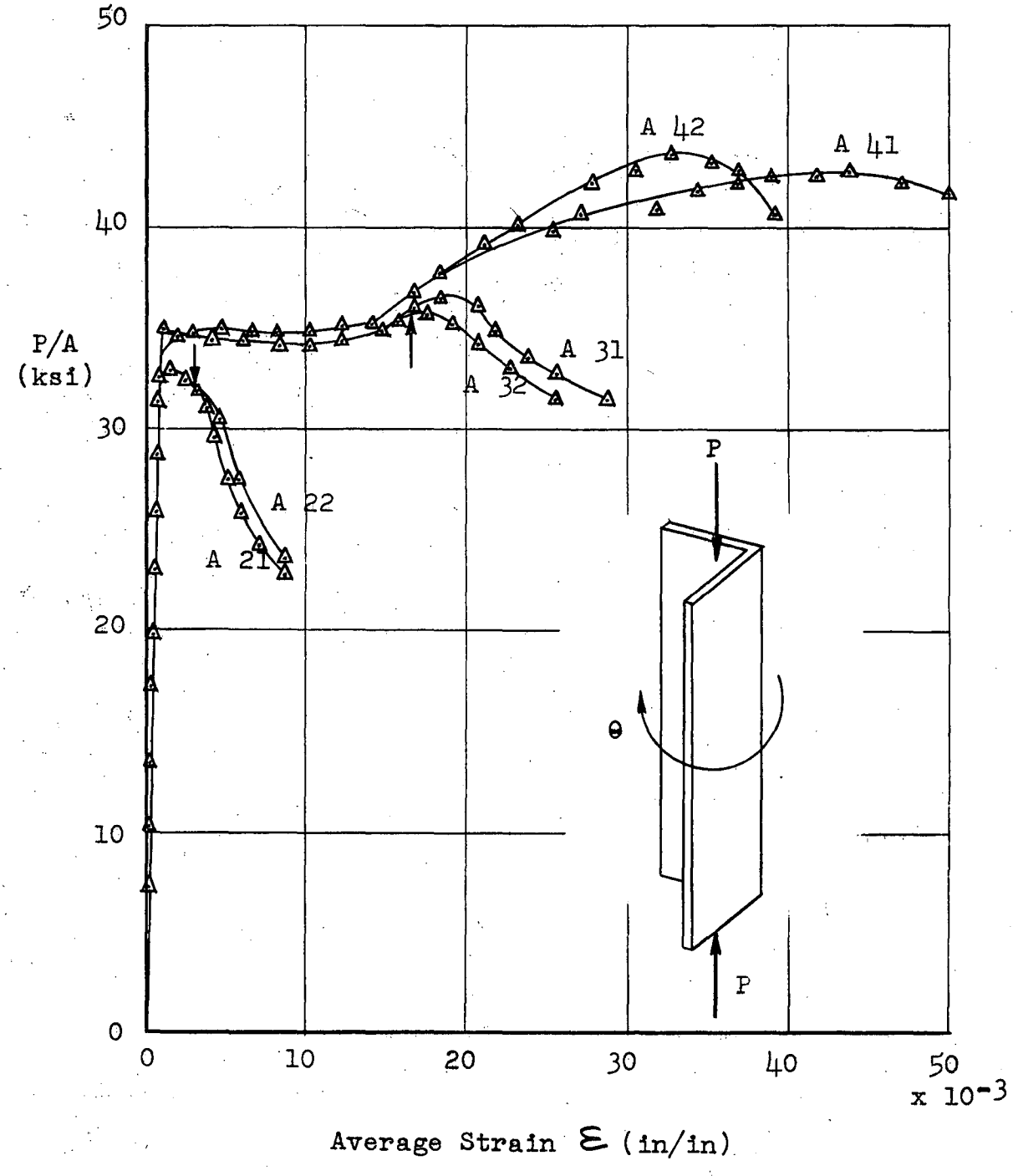

FIG. 28 RESULTS OF ANGLE COMPRESSION TESTS

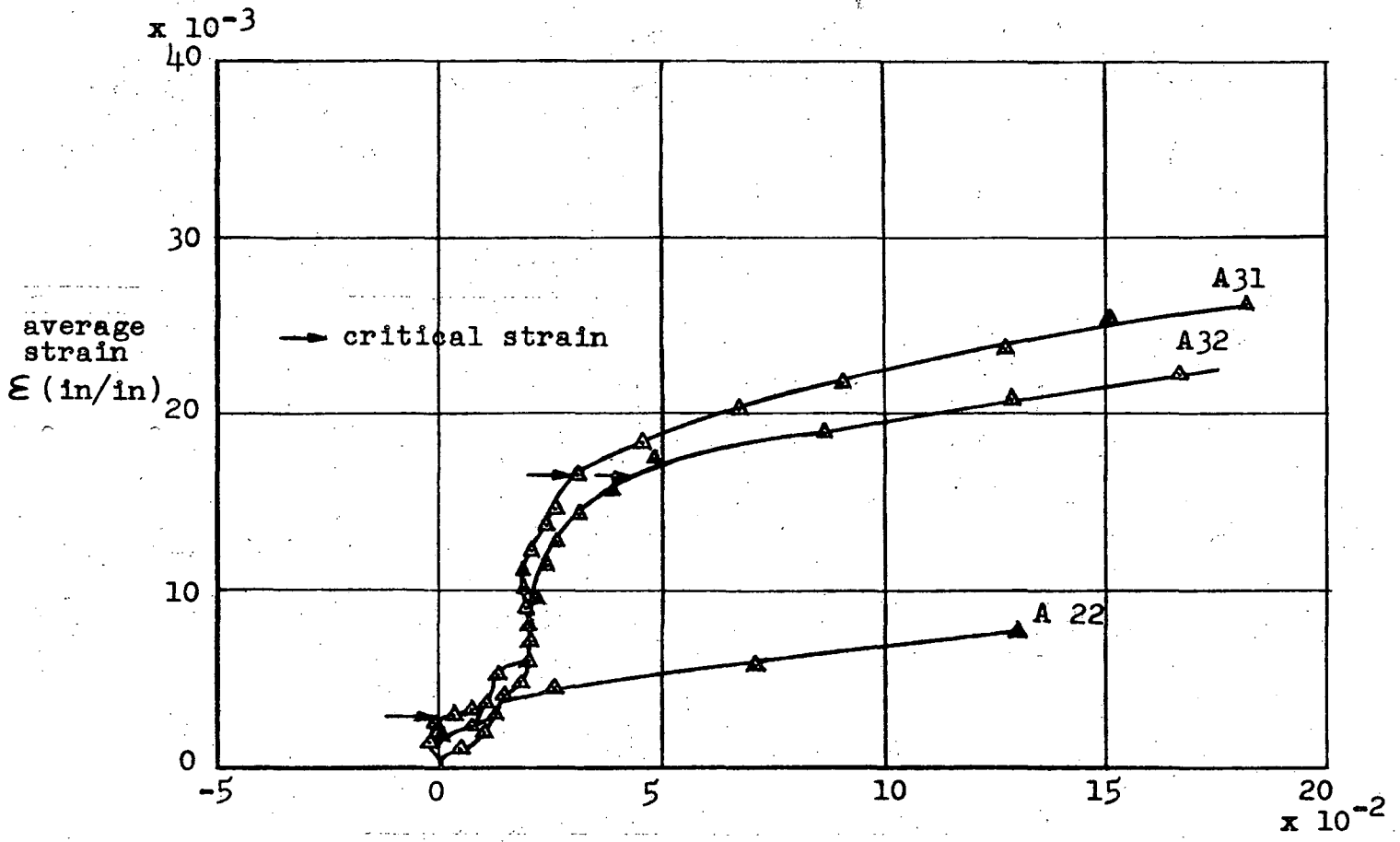

FIG. 29 ROTATION OF ANGLE SPECIMENS

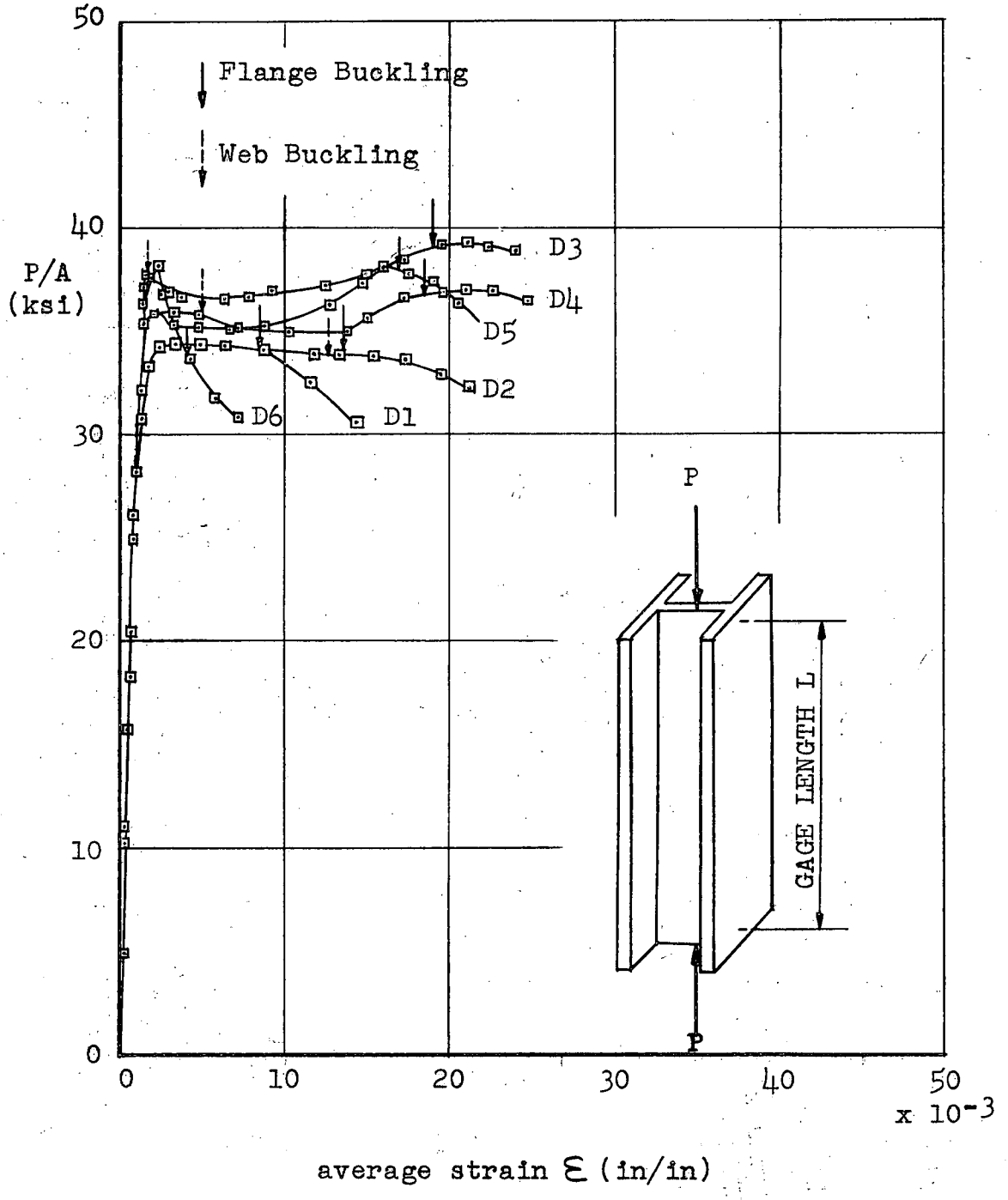

FIG. 30 RESULTS OF WF COMPRESSION TESTS

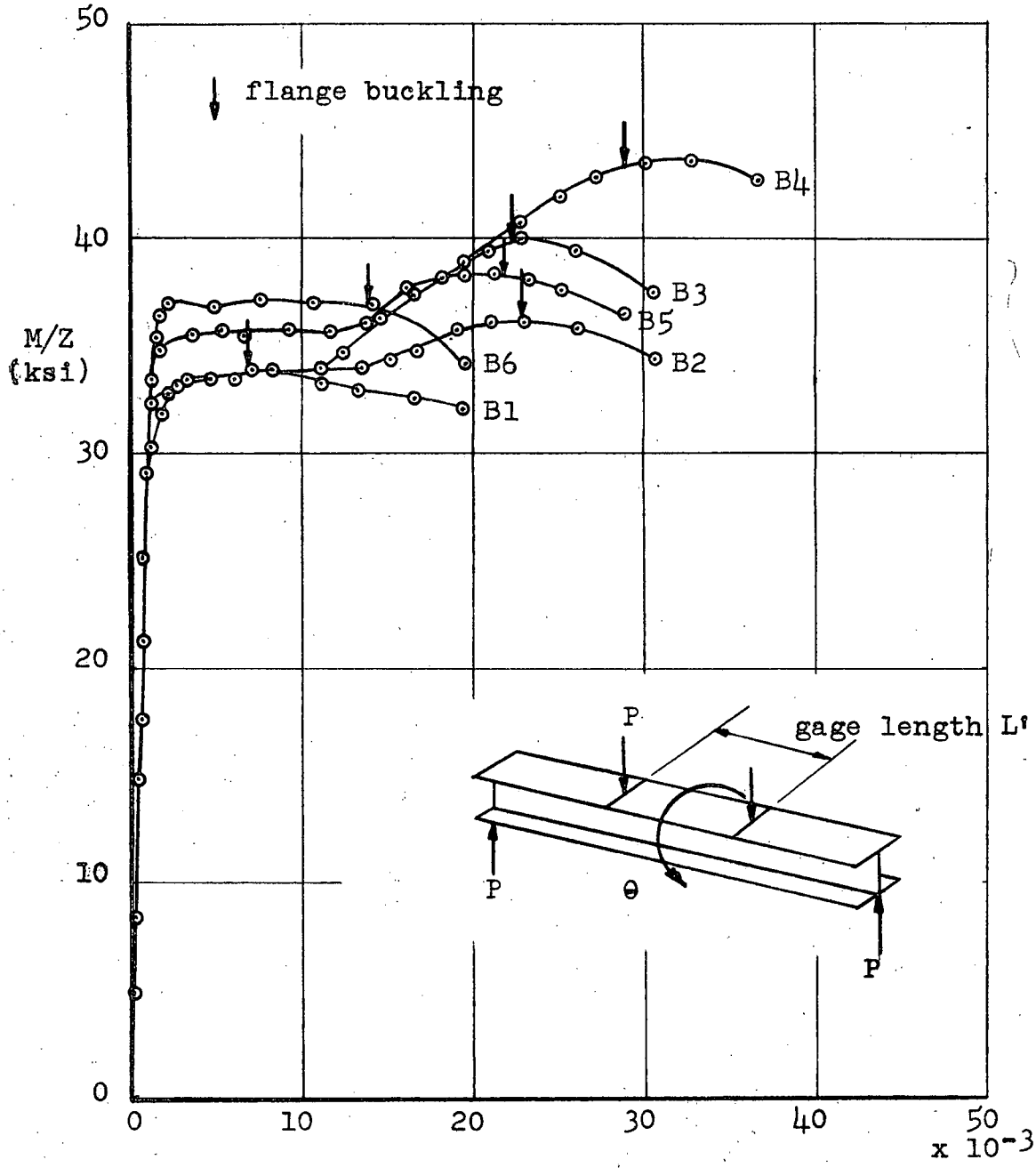

FIG. 31 RESULTS OF WF BENDING TESTS

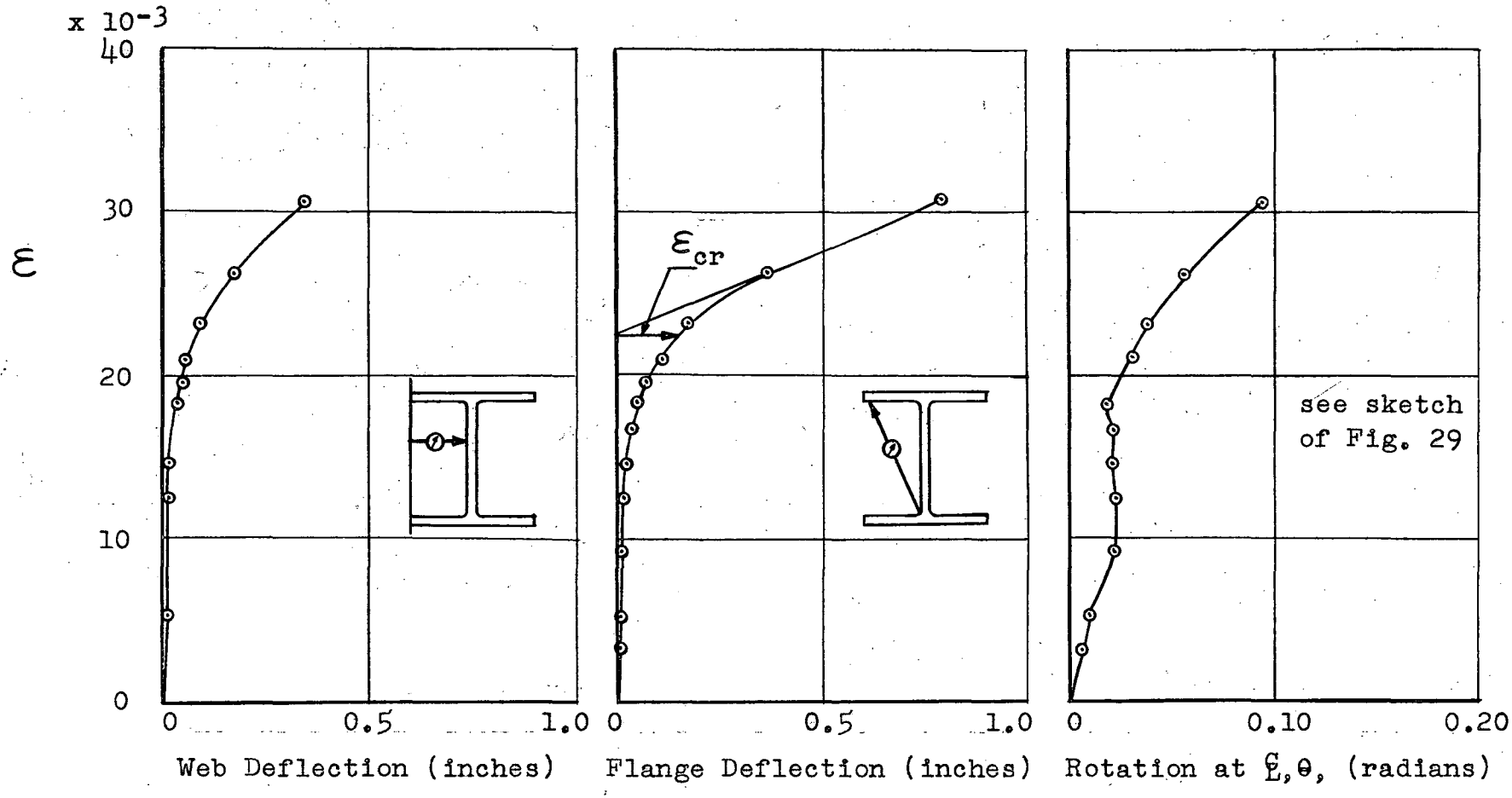

FIG. 32 TYPICAL CURVES FOR LATERAL WEB AND FLANGE DEFLECTIONS AND LATERAL ROTATION (WF BENDING TEST B3)

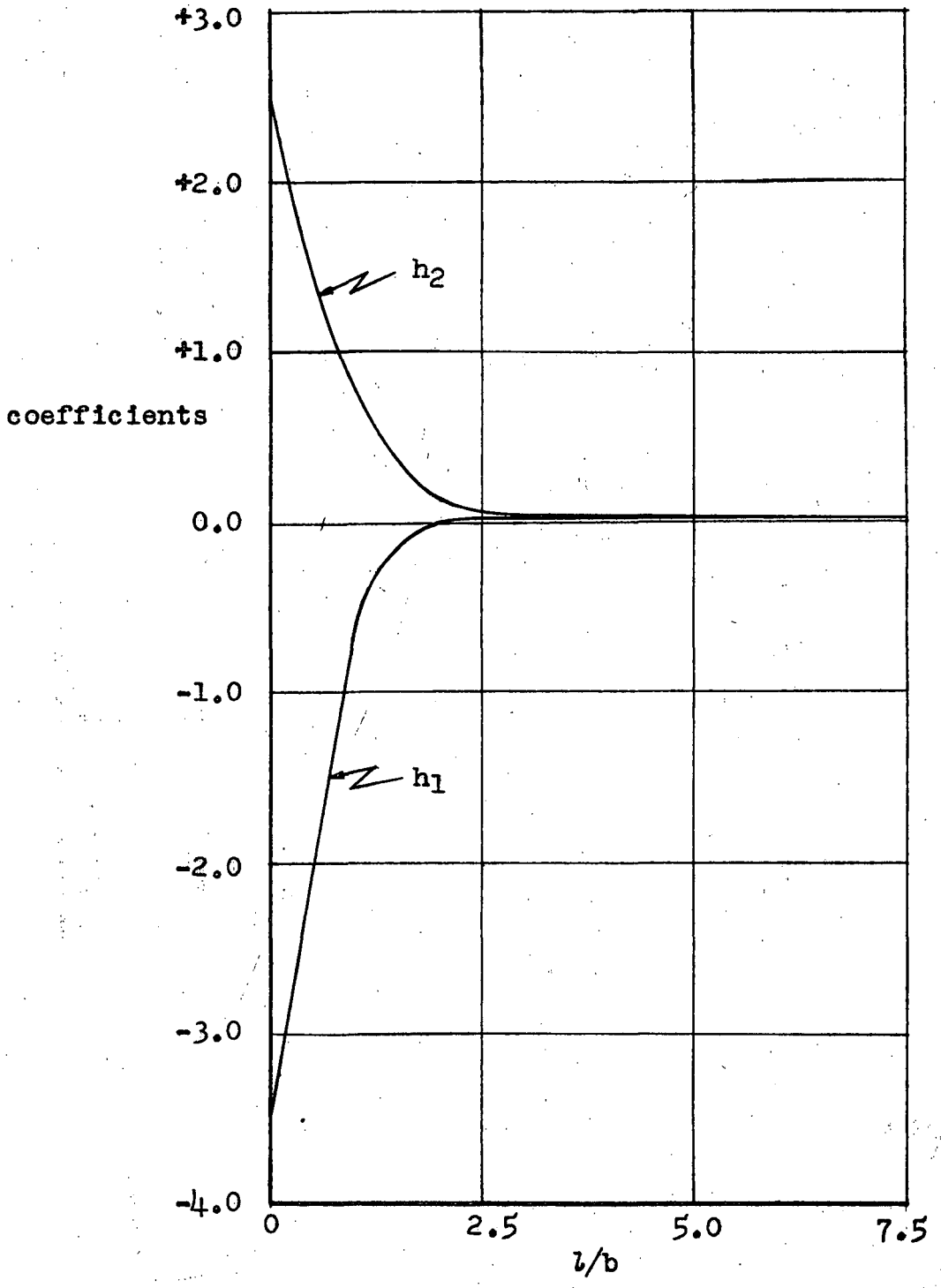

FIG. 33 COEFFICIENTS OF DEFLECTION SURFACE FOR HINGED FLANGE, h_1 and h_2

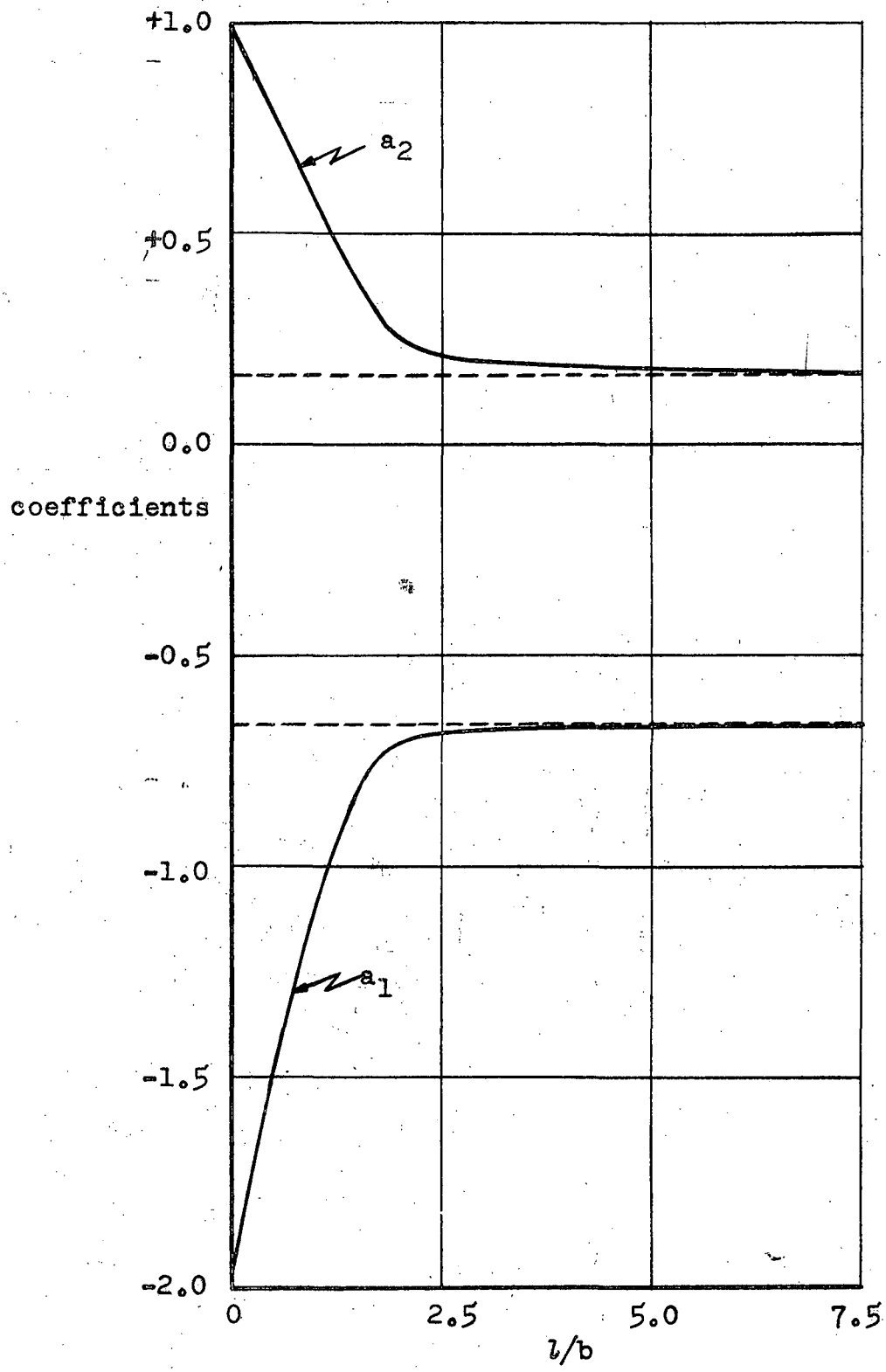

FIG. 34 COEFFICIENTS OF DEFLECTION SURFACE FOR FIXED FLANGE, a_1 and a_2

V I T A

The author, eldest son of Jan and Hinderkien Haaijer, was born on April 26, 1929 in Borger, The Netherlands.

He entered the Technological University of Delft, The Netherlands in September, 1947. Upon completion of his program of studies the degree of Civil Engineer was awarded in November, 1952. During 1951 and 1952 he was employed as assistant to Professor N. Nanninga, Professor of foundation engineering at the Delft University.

In September 1952 he came to Lehigh University, Bethlehem, Pennsylvania. Besides being engaged in research at Fritz Engineering Laboratory he taught in the Division of Mechanics.

During leaves of absence from Lehigh University he worked as bridge designer with Gannett, Fleming, Corddry and Carpenter, Inc., Consulting Engineers, Harrisburg, Pennsylvania and as research engineer at the Hydraulics Laboratory, Delft, The Netherlands.

On January 29, 1955 he married Willemina K. Veenstra. Presently they have one daughter, Karen, born November 21, 1955.